JOURNAL OF VIROLOGY, Nov. 1997, p. 8602–8614 Vol. 71, No. 11
0022-538X/97/$04.00+0

Mutational Analysis of the Herpes Simplex Virus Type 1 ICP0 C_3HC_4 Zinc Ring Finger Reveals a Requirement for ICP0 in the Expression of the Essential α27 Gene

ERIK K. LIUM[1] AND SAUL SILVERSTEIN[1,2]*

Integrated Program in Cellular, Molecular and Biophysical Studies[1] and Department of Microbiology,[2] College of Physicians and Surgeons, Columbia University, New York, New York 10032

Received 19 May 1997/Accepted 15 July 1997

The herpes simplex virus type 1 (HSV-1) immediate-early (IE) protein ICP0 has been implicated in the regulation of viral gene expression and the reactivation of latent HSV-1. Evidence demonstrates that ICP0 is an activator of viral gene expression yet does not distinguish between a direct or indirect role in this process. To further our understanding of the function of ICP0 in the context of the virus life cycle, site-directed mutagenesis of the consensus C_3HC_4 zinc finger domain was performed, and the effects of these mutations on the growth and replication of HSV-1 were assessed. We demonstrate that alteration of any of the consensus C_3HC_4 cysteine or histidine residues within this domain abolishes ICP0-mediated transactivation, alters the intranuclear localization of ICP0, and significantly increases its stability. These mutations result in severe defects in the growth and DNA replication of recombinant herpesviruses and in their ability to initiate lytic infections at low multiplicities of infection. These viruses, at low multiplicities of infection, synthesize wild-type levels of the IE proteins ICP0 and ICP4 at early times postinfection yet exhibit significant decreases in the synthesis of the essential IE protein ICP27. These findings reveal a role for ICP0 in the expression of ICP27 and suggest that the multiplicity-dependent growth of α0 mutant viruses results partially from reduced levels of ICP27.

Herpes simplex virus type 1 (HSV-1) and type 2 (HSV-2) infections proceed from a primary lytic infection in the periphery to a lifelong state of latency in sensory neurons, characterized by episodes of virus reactivation and lytic infection. The regulatory mechanisms that control HSV gene expression, the establishment and maintenance of latency, and the reactivation of latent virus are complex and involve interactions between host- and virus-specific factors.

The genes of HSV-1 and HSV-2 are classified into three kinetic classes, immediate-early (α), early (β), and late (γ), based on their temporal expression during productive infections (37, 38, 61). The immediate-early genes (α0, α4, α27, α22, α47, and αX) are the first to be transcribed after infection (references 5 and 61 and references therein). Subsequent expression of early genes, whose products are largely involved in replication of the virus genome, and late genes, which encode many of the structural components of the HSV virion, requires the prior synthesis of α gene products (14, 15, 36, 57). Three of the α gene products, infected-cell proteins 0, 4, and 27 (ICP0, ICP4, and ICP27), cooperatively regulate the expression of all kinetic classes of virus genes (23, 30, 47, 52, 56–58, 62, 76, 78). ICP4 is an essential protein that functions as both a repressor and an activator of transcription. In concert with ICP0, ICP4 activates the expression of early and late genes while repressing its own expression, as well as that of the α0 gene (14, 32, 42, 43, 51, 57, 60). ICP27, another essential protein, is required for the expression of β and γ genes during the HSV life cycle. This protein appears to act primarily at the posttranscriptional level (47, 59, 62, 65, 67, 73); however, recent evidence supports a more direct role for ICP27 in the regulation of gene expression (55).

The events that control HSV latency and the balance between the lytic and latent state are not clear. Latent HSV-1 and HSV-2 appear to express primarily the latency-associated transcripts, whose function(s) is unknown (26, 69). Current evidence suggests that ICP0 functions in the reactivation of latent HSV-1, since it was shown to be both necessary and sufficient for the reactivation of latent virus in model systems (33, 82).

ICP0 is a 775-amino-acid nuclear phosphoprotein with an apparent molecular mass of 110 kDa (56, 78). It has been shown to increase the expression of reporter genes from a diverse range of viral and cellular gene promoters in transient-expression assays. However, these experiments do not differentiate between a direct and/or indirect role for ICP0 in the activation of transcription (9, 12, 19, 21, 22). Mutational analyses of ICP0, in transient-expression assays and in the context of the virus genome, identified regions that are essential for transcriptional activation and wild-type virus growth kinetics (9, 11, 12, 19–21, 70). One such region contains a consensus C_3HC_4 zinc finger motif (4, 24), a zinc-binding domain found in a functionally diverse set of proteins with roles in transcription, differentiation, oncogenesis, DNA repair, and recombination (27, 28).

All alphaherpesviruses for which the DNA sequence is available encode proteins related to HSV-1 ICP0 (27). Although the function(s) of these proteins has yet to be established, they all appear to participate in the regulation of virus gene expression (11, 12, 19, 20, 22, 33, 48, 49, 74, 79, 82). Structural analysis of the C_3HC_4 zinc finger domain from one of these proteins, the product of equine herpesvirus gene 63 (EHV-63), demonstrates that this domain conforms to a ββαβ structure, comprising three antiparallel beta-strands and an amphipathic alpha-helix (4, 24). This domain does not appear to bind DNA or RNA in vitro (24). Mutagenesis of the HSV-1 ICP0 C_3HC_4 domain, and swaps between this domain and its homolog, EHV-63, suggest that these two domains may perform similar functions (4, 18).

This report presents a detailed mutational analysis of the C_3HC_4 domain of HSV-1 ICP0. Evidence is provided that the

* Corresponding author. Phone: (212) 305-8149. Fax: (212) 305-5106. E-mail: sjs6@columbia.edu.

consensus C_3HC_4 cysteines and histidine are essential for ICP0 function in the context of a productive infection and in transient-expression assays. We further demonstrate that ICP0 is required for efficient expression of the essential IE gene product ICP27 in low-multiplicity infections. Our results support the conclusion that ICP0 functions as an initiator of the productive virus life cycle and that in the absence of functional ICP0, the probability of establishing a lytic herpesvirus infection at low multiplicities is dramatically reduced.

MATERIALS AND METHODS

Cells and viruses. Vero cells were maintained in Dulbecco's modified Eagle's medium (DMEM) (Gibco BRL, Grand Island, NY) supplemented with 5% bovine calf serum (Hyclone Laboratories Inc., Logan, Utah). 0-28 (63) and L7 (64) cells are derivatives of Vero cells that express the HSV-1 α0 gene under the control of its cognate promoter. These cells were maintained in DMEM supplemented with 5% bovine calf serum and 500 μg of G418 per ml. U2OS cells (80) were maintained in the same manner as Vero cells. 293T cells (16) were maintained in DMEM supplemented with 10% fetal calf serum. The media were supplemented with 100 U of penicillin per ml and 100 μg of streptomycin (Gibco BRL) per ml unless otherwise noted. The viruses used in this study were wild-type HSV-1 (Glasgow strain 17), IE-0:LacZ and vCM2/7 (11), vCPc0 (55), *dl*1403 (70), and the α0 mutant viruses vC116G, vH126A, and vC116G/C156A (this study).

Plasmid DNAs. Plasmid pSS7 contains the α0 gene from HSV-1 (KOS) (31). Plasmid pDS17, which contains the α0 cDNA (81) and associated regulatory sequences, was constructed by replacing the *Mlu*I-*Eco*RI fragment of pDS16 (81) with the corresponding fragment from p0XB (12). Plasmid pCM2/7 has been described previously (11). Plasmid pDSE-17B was created by destruction of the *Asp*718 site located 3′ of the HSV-1 sequences in pDS17. Plasmid pIBI31-0-103/214 contains the *Xho*I-*Asp*718 fragment of the α0 cDNA (81), which encodes the ICP0 C_3HC_4 zinc finger motif, in pIBI31. Construction of plasmids pT/A-C116G, pT/A-C119G, pT/A-H126A, pT/A-C129G, pT/A-C129H, pT/A-C134G, pT/A-H136A, pT/A-C139A, pT/A-C142G, pT/A-C153A, and pT/A-C156A is described below. Plasmids pEL0-C116G, pEL0-C119G, pEL0-H126A, pEL0-C129G, pEL0-C134G, pEL0-C153A, and pEL0-C156A were constructed by replacing the *Xho*I-*Asp*718 fragment of the α0 cDNA in pDSE-17B with the corresponding α0 C_3HC_4 mutant fragment from pT/A-C116G, pT/A-C119G, pT/A-H126A, pT/A-C129G, pT/A-C134G, pT/A-C153A, or pT/A-C156A, respectively. Plasmids pEL0-C129H, pEL0-H136A, pEL0-C139A, and pEL0-C142G were constructed by replacing the *Xho*I-*Mun*I fragment of the α0 cDNA in pDSE-17B with the corresponding C_3HC_4 mutant fragment from pT/A-C129H, pT/A-H136A, pT/A-C139A, or pT/A-C142G, respectively. Plasmid pEL0-C116G/C156A was constructed by replacing the *Mun*I-*Mlu*I fragment of pEL0-C116G with the corresponding fragment from pEL0-C156A. Plasmid pIGA103 contains the HSV-1 α4 promoter (−323 to +32) in pIC20H (29). Plasmid pCPC-4P-luc (53), containing the firefly luciferase gene under the control of the HSV-1 α4 promoter (−323 to +32), was constructed by insertion of the *Bam*HI fragment of p19luc (75) into pIGA103. ptk-LUC, containing the firefly luciferase gene under the control of the HSV-1 thymidine kinase promoter (−200 to +58), has been described previously (50). pEL-PgC-luc, containing the firefly luciferase gene under the control of the HSV-1 glycoprotein C promoter (−1339 to +34), was constructed by insertion of the *Bam*HI fragment of p19luc (75) into pTB2 (12).

Mutagenesis. Sequential PCR mutagenesis of the *Xho*I-*Asp*718 fragment of the α0 cDNA (81) was performed as described previously (3) with minor modifications. The sequences of the primers (Columbia University Cancer Center, New York, N.Y. or Genset Corp., La Jolla, Calif.) used are as follows. Flanking: pIBI31-0-103/214 5′3′, 5′-ACCGCCTCTCCCCGCGCGTT-3′; pIBI31-0-103/214 3′5′, 5′-GGGGAAAGCCGGGGAACGTG-3′. Mutagenic: C116 5′3′, 5′-GGCGACGTGGGCGCCGTGTG-3′; C116 3′5′, 5′-CACACGGCGCCCACGTCGCC-3′; C119 5′3′, 5′-GCGCCGTGGGGACGGATGAG-3′; C119 3′5′, 5′-CTCATCCGTCCCCACGGCGC-3′; H126 5′3′, 5′-ATCGCGCCCGCCCTGCGCTG-3′; H126 3′5′, 5′-CAGCGCAGGGCGGGCGCGAT-3′; C129 5′3′, 5′-CCTGCGCGGCGACACCTTCC-3′; C129 3′5′, 5′-GGAAGGTGTCGCCGCGCAGG-3′; C129H 5′3′, 5′-CCTGCGCCACGACACCTTCC-3′; C129H 3′5′, 5′-GGAAGGTGTCGTGGCGCAGG-3′; C134 5′3′, 5′-CCTTCCCGGGCATGCACCGC-3′; C134 3′5′, 5′-GCGGTGCATGCCCGGGAAGG-3′; H136 5′3′, 5′-CGTGCATGGCGCGCTTCTGC-3′; H136 3′5′, 5′-GCAGAAGCGCGCCATGCACG-3′; C139 5′3′, 5′-ACCGCTTCGCGATCCCGTGC-3′; C139 3′5′, 5′-GCACGGGATCGCGAAGCGGT-3′; C142 5′3′, 5′-CATCCCGGGCATGAAAACCT-3′; C142 3′5′, 5′-AGGTTTTCATGCCCGGGATG-3′; C153 5′3′, 5′-CGCAACACCGCCCCGCTGTG-3′; C153 3′5′, 5′-CACAGCGGGGCGGTGTTGCG-3′; C156 5′3′, 5′-CCTGCCCGCTGGCCAACGCC-3′; C156 3′5′, 5′-GGCGTTGGCCAGCGGGCAGG-3′.

Primary PCR amplification mixtures contained 1 ng of pIBI31-0-103/214, 150 nM mutagenic primer, 150 nM flanking primer, 200 μM deoxynucleoside triphosphates (Pharmacia Biotech, Uppsala, Sweden), 10 mM Tris-HCl (pH 9.0), 50 mM KCl, 1.5 mM $MgCl_2$, 1% Triton X-100, 7.5% glycerol, 1 mM spermidine (pH 7.0), and 2 U of *Taq* DNA polymerase (Promega, Madison, Wis.). Primary PCR products were purified on Qiaquick Spin columns (Qiagen, Chatsworth, Calif.). Secondary PCR amplifications were performed as above, with minor modifications. Reaction mixtures contained 750 nM flanking primers (pIBI31-0-103/214 5′3′ and pIBI31-0-103/214 3′5′) and 5% (50 to 100 ng) of each sibling primary amplification product. Secondary amplimers were ligated into pGEM-T (Promega) to create plasmids pT/A-C116G, pT/A-C119G, pT/A-H126A, pT/A-C129G, pT/A-C129H, pT/A-C134G, pT/A-H136A, pT/A-C139A, pT/A-C142G, pT/A-C153A, and pT/A-C156A. The DNA sequences of the cloned fragments (*Xho*I-*Asp*718) were verified by cycle sequencing with AmpliCycle (Perkin-Elmer, Foster City, Calif.). The mutated C_3HC_4 domain coding sequences were introduced into the α0 cDNA in pDSE-17B, as described above.

Transient-expression assays. (i) Transfection. Transfections were performed by the calcium phosphate method as described previously (55, 77), with the addition of a 1-min glycerol shock with 1 ml of 15% glycerol in HEPES-buffered saline (3). All transfection mixtures contained a total of 15 μg of DNA: 1 μg of the indicated luciferase reporter plasmid; 0, 0.1 (data not shown), or 1 μg of the indicated wild-type or mutant α0 cDNA; and carrier plasmid.

(ii) Transient-expression assays. Transfected Vero cell monolayers were harvested at 48 h posttransfection. Luciferase activity was quantified with a Berthold Lumat LB9501 luminometer (Wallac Inc., Gaithersburg, Md.), as described previously (7). Luciferase activities were determined from triplicate transfections in two independent experiments.

Western blot analyses. (i) Transfected cells. Vero cells were transfected with 15 μg of plasmid DNAs, as described above. 293T cells were transfected, as previously described (55), with 15 μg of DNA. At 48 h posttransfection, the cells were scraped into ice-cold phosphate-buffered saline (PBS) and collected by centrifugation at 4°C. Cell pellets were solubilized in 300 μl (Vero) or 600 μl (293T) of 1.5× sodium dodecyl sulfate-polyacrylamide gel electrophoresis (SDS-PAGE) sample buffer (41) and boiled for 10 min. The proteins were separated by SDS-PAGE (41) and transferred to nitrocellulose membranes (72). Immunodetection of ICP0 was performed as previously described (54) with rabbit polyclonal antibody CLU7 (43). The relative levels of ICP0 were quantified by densitometric analysis using an AGFA ARCUS II scanner and NIH Image 1.51.

(ii) Infections. Western blot analysis of virus-specified proteins was performed as described previously (43), with one addition. HSV-1 VP5 was detected with rabbit polyclonal antibody NC-1 (provided by G. Cohen, Department of Microbiology, University of Pennsylvania). The proteins were quantified by densitometric analysis using an AGFA ARCUS II scanner and NIH Image 1.51.

Immunofluorescence. (i) Transfections. Vero cells were transfected with 0.5, 2, or 15 μg of plasmid DNAs encoding the indicated wild-type or mutant form of ICP0, as described above. Carrier plasmid DNA was used to adjust all transfection mixtures to contain a total of 15 μg of DNA. At 48 h posttransfection, the cell monolayers were rinsed with PBS, fixed with 3.7% formaldehyde in PBS for 30 min, permeabilized with 100% acetone at −20°C for 10 min, and stored at 4°C in PBS. Immunodetection of ICP0 was performed with polyclonal antibody CLU7 (43), diluted 1:200 in PBS. Fluorescein isothiocyanate-conjugated secondary goat anti-rabbit immunoglobulin G antibodies (Kirkegaard and Perry, Gaithersburg, Md.) were diluted 1:200. Preparations were viewed under a Leitz Dialux microscope with optical systems for the selective visualization of fluorescein. Representative fields of cells were photographed with Ektachrome P1600 film (Eastman Kodak, Rochester, N.Y.), using a Nikon UFX-DXII photographic system.

(ii) Fluorescent-focus assays. Fluorescent-focus assays were performed as previously described (11), with minor modifications. Briefly, Vero cells were infected at a multiplicity of infection (MOI) of 0.01 with wild-type HSV-1 or the α0 mutant virus vC116G, vH126A, or vC116G/C156A. At 8 h postinfection, ICP0 was detected by indirect immunofluorescence, as described above. The relative particle-to-PFU ratios of these viruses were calculated from the number of positively staining cells at 8 h postinfection relative to the titer of each virus on L7 cells.

(iii) Virus spread. Vero cells were seeded in 60-mm plates on sterile glass coverslips and infected at a MOI of 0.01 with wild-type HSV-1 or the α0 mutant virus vC116G, vH126A, or vC116G/C156A. The cells were fixed and permeabilized at the indicated times postinfection, and ICP0 was detected by indirect immunofluorescence, as described above.

Construction of α0 mutant viruses. (i) Transfections. Vero cells were transfected as previously described (43). Transfection mixtures contained 12.5 μg of plasmid DNA (pEL0-C116G, pEL0-H126A, or pEL0-C116G/C156A), linearized with *Hin*dIII, and 100 PFU of IE-0:LacZ nucleocapsids (66). vCPc0 (55) and vCM2/7 (11) have been described.

(ii) Purification of recombinant viruses. Recombinant herpesviruses with mutations in the α0 gene were generated as previously described (43). The site-directed mutations in the α0 C_3HC_4 domain were verified by direct sequence analysis of PCR-amplified virus DNAs, as described below.

Analysis of virus DNAs. (i) DNA preparation. Virus DNAs were prepared for PCR and Southern blot analysis as previously described (35, 43).

(ii) Amplification and sequencing of recombinant α0 viruses. The site-directed mutations in the recombinant virus DNAs were verified by direct PCR sequencing of 195-bp PCR amplimers of the α0 cDNA. The sequences of the primers used for PCR amplification and sequencing are as follows: 3337U, 5′-CCTCGAGAGGACGGGGGGAGC-3′; 3510L, 5′-GCGTCACGCCCACTATCAGGTAC-3′.

(iii) DNA probes. The probes used throughout this study consisted of the 5.2-kb *Sst*I-*Asp*718 fragment of the α0 gene (−810 to +4382) and the 4.5-kb *Sal*I-*Dde*I fragment of the α4 gene. The probes were labeled with [α-^{32}P]dCTP (3,000 Ci/mmol; DuPont NEN, Boston, Mass.) by random priming (Boehringer Mannheim, Indianapolis, Ind.).

(iv) Southern blot analysis. Infected-cell DNA was digested with *Sac*I and *Pst*I or with *Not*I and *Pst*I. Digested DNAs were separated by agarose gel electrophoresis and transferred to SS-Nytran filters (Schleicher & Schuell, Keene, N.H.). Southern blot hybridization with a 5.2-kb α0 probe (−810 to +4382) was performed as specified by the manufacturer. The blots were washed as recommended and exposed to Biomar Blue film.

Virus growth assays. (i) Burst size. Burst size analysis was performed with two independent isolates for each of the recombinant α0 viruses (vC116G, vH126A, and vC116G/C156A) as previously described (43). The titers of all viruses were determined prior to analysis by using the ICP0-complementing cell line L7 (64). Virus yields at 2 and 24 h postinfection were determined by titrating on L7 cells.

(ii) Growth curves. The titers of all virus stocks (HSV-1 strain 17, vCPc0, vCM2/7, vC116G, vH126A, vC116G/C156A, and *dl*1403) were determined prior to growth analysis by titrating on the ICP0-complementing cell line L7 (64). Vero cells were infected at a MOI of either 0.1 or 10, and the virus yields were determined as previously described (43) on L7 cells. Growth curves represent the average of three independent infections, each titrated in duplicate.

DNA replication and genome-to-PFU ratios. (i) Replication. Vero cells (10^6) were infected at a MOI of either 0.1 or 10. Infections were halted by freezing (−80°C) at 1 and 16 h postinfection, and total infected-cell DNAs were prepared as described previously (43). Equivalent amounts of infected-cell DNAs were blotted to GeneScreen Plus by using a MINIFOLD II Slot-Blot System (Schleicher & Schuell), and cross-linked by UV irradiation with a Stratalinker 2400 (Stratagene, La Jolla, Calif.). The virus DNAs were hybridized, as specified by the manufacturer, with a 4.5-kb fragment of the HSV-1 α4 gene, described above. The blots were washed as recommended and visualized by autoradiography. Virus replication was quantified by PhosphorImager analysis (Molecular Dynamics PhosphorImager 445SI) with ImageQuaNT software.

(ii) Genome-to-PFU ratios. The genome-to-PFU ratios (10) were determined by comparing the amount of HSV-1 DNA in infected cells at 1 h postinfection to the number of PFU per ml for the corresponding virus. These values were then compared to the genome/PFU ratio of wild-type HSV-1. Briefly, Vero cells were infected at a MOI of 10, and infected-cell DNAs were prepared at 1 h postinfection as described previously (43). Virus DNAs were quantified by hybridization and PhosphorImager analysis, as described above.

Extraction of ICP0 from infected cells. Vero cells (3×10^6) were infected at an MOI of 0.5 or 40. At 8 h postinfection the infected-cell monolayers were rinsed twice with 5 ml of ice-cold PBS and scraped into 600 μl of ICP0 lysis buffer containing 20 mM HEPES-KOH (pH 7.5), 0.25% Nonidet P-40 (vol/vol), 400 mM NaCl, 10 mM $MgCl_2$, 10% (vol/vol) glycerol, 50 μg of DNase I per ml, 50 μg of RNase I per ml, 1 mM phenylmethylsulfonyl fluoride, 0.1 mM L-1-chloro-3-(4-tosylamido)-4-phenyl-2-butanone (TPCK), and 0.1 mM L-1-chloro-3-(4-tosylamido)-7-amino-2-heptanone (TLCK) (Boehringer Mannheim). The cell lysates were incubated for 20 min at 4°C, sonicated for 2 min with a Sonifier 450 (Branson, Danbury, Conn.), and clarified by centrifugation at 16,000 × *g* for 15 min at 4°C. The pellets and the supernatants were solubilized in 1.5× SDS-PAGE sample buffer (41), and the levels of ICP0 and ICP27 in these fractions were determined by Western blot analysis, as described above.

Immunoprecipitation of ^{35}S-labeled ICP0, ICP4, and ICP27. (i) ^{35}S labeling. Vero cells were infected at a MOI of 0.5. At the indicated times postinfection, the cell monolayers were rinsed twice with Met-free DMEM (Gibco BRL) and incubated at 37°C for 30 min in the presence of 200 μCi of Trans^{35}S Label (ICN Pharmaceuticals Inc., Costa Mesa, Calif.) in 500 μl of Met-free DMEM supplemented with 1% dialyzed bovine calf serum. Infected-cell lysates were prepared as described above for the extraction of ICP0.

(ii) Pulse-chase. Vero cells were infected at a MOI of 0.5 and labeled with Trans^{35}S Label for 30 min at 2.5 h postinfection, as described above. At 3 h postinfection, the infected-cell monolayers were rinsed twice with DMEM and chased for 0, 2, or 4 h. Following the chase, infected-cell lysates were prepared as described above for the extraction of ICP0.

(iii) Immunoprecipitation. Infected-cell lysates (200 μl) and 3 μl of antibody to ICP0 (CLU7), ICP4 (1114), or ICP27 (CLU38) (43) were mixed for 1 h at 4°C prior to the addition of 25 μl of a 50% (vol/vol) suspension of GammaBind Plus Sepharose (Pharmacia) in ICP0 lysis buffer, and the mixtures were incubated for another 1 h at 4°C with constant mixing. The beads were washed three times with RIPA buffer (10 mM Tris-HCl [pH 8.0], 150 mM NaCl, 1% Triton X-100 [vol/vol], 1% sodium deoxycholate, 0.1% SDS, 1 mM phenylmethylsulfonyl fluoride, 0.1 mM TPCK, 0.1 mM TLCK) for 15 min at 4°C, resuspended in 25 μl of 2× SDS-PAGE sample buffer (41), and boiled for 10 min. The proteins were separated by SDS-PAGE and visualized by either fluorography using Entensify (DuPont NEN) or PhosphorImager analysis. We note that this procedure results in the quantitative immunoprecipitation of ICP0, ICP4, and ICP27 from infected-cell extracts. The relative levels of ICP0, ICP4, and ICP27 were determined by PhosphorImager analysis using ImageQuaNT software.

Analysis of infected-cell RNAs. (i) RNA preparation. Vero cells were infected at a MOI of 0.5, and total infected-cell RNAs were prepared by using the High Pure RNA isolation kit (Boehringer Mannheim) as specified by the manufacturer.

(ii) RT-PCR. The abundance of α0, α4, and α27 RNAs in HSV-1-infected cells was determined by coupled reverse transcription-PCR (RT-PCR) with the EZ r*Tth* RNA PCR kit as specified by the manufacturer (Perkin-Elmer), with modifications. Briefly, reaction mixtures contained 65 nM [α-^{32}P]dCTP (3,000 Ci/mmol) and 900 nM of primer (0-RF3′5′, 4-2, or ICP27-L-RT [see below]). RT was performed in the presence of only primers complementary to the α0, α4, and α27 RNAs (0-RF3′5′, 4-2, or ICP27-L-RT). Following reverse transcription, secondary primers for PCR (0-RF5′3′, 4-1, or ICP27-U-RT) were added to the corresponding reaction mixtures. The number of PCR cycles for these amplifications was 20, as the amplification of the α0, α4, and α27 RNAs was determined to be linear under our conditions through ≤28 PCR cycles. The absence of contaminating DNA in each RNA sample was demonstrated by performing PCR in the absence of RT. The sequences of the primers used in this analysis are as follows: 0-RF5′3′, 5′-GAGGAAGACCCCGGCAGTTGCG-3′; 0-RF3′5′, 5′-GCGTCACGCCCACTATCAGGTAC-3′; 4-1, 5′-CGACACGGATCCACGACCCGAC-3′; 4-2, 5′-GATCCCCCTCCCGCGCTTCGTC-3′; ICP27-U-RT, 5′-AGCCGCCGCGACGACCTGGAA-3′; ICP27-L-RT, 5′-CTGTGGGGCGCTGGTTGAGGAT-3′. The DNA sequences of 4-1 and 4-2 are similar to those described previously (40). These primers result in the amplification of a 228-bp fragment of the α0 RNA, a 100-bp fragment of the α4 RNA, and a 220-bp fragment of the α27 RNA. The reaction products were quantified by PhosphorImager analysis, as described above.

RESULTS

Experimental design. The C_3HC_4 domain of HSV-1 ICP0 is distinguished from the related domains of several ICP0 homologs (27) by the presence of two nonconsensus amino acids with the potential to coordinate zinc, histidine 126, and cysteine 129 (Fig. 1). The positions of these amino acids, as well as their potential to participate in the coordination of zinc, suggested that the C_3HC_4 domain of HSV-1 ICP0 could represent an alternative C_3HC_4 zinc finger (4, 27) (Fig. 1). Thus, the objective of this study was to determine (i) whether these nonconsensus amino acids are important for the structure and/or function of the C_3HC_4 domain and (ii) which cysteines and histidine(s) within this domain are essential for ICP0 function. Additionally, we further characterized the role of ICP0 in the growth and replication of HSV-1. Accordingly, each of the cysteine and histidine residues within the C_3HC_4 domain were altered by mutagenesis, and the effects of these mutations on ICP0 function were assessed in transient-expression assays and in the context of a productive virus infection.

Mutagenesis. Sequential PCR mutagenesis of the *Xho*I-*Asp*718 fragment of the α0 cDNA (81) was performed to change each of the cysteine or histidine residues in the ICP0 C_3HC_4 domain to either an alanine (A), glycine (G), or histidine (H) (Fig. 1). The predicted DNA sequences of these mutant fragments of the α0 gene were verified, and the fragments were introduced into the α0 cDNA (81). The resulting mutant cDNA constructs encode the following single amino acid changes within the C_3HC_4 domain: C116G, C119G, H126A, C129G, C129H, C134G, H136A, C139A, C142G, C153A, or C156A (Fig. 1). The double mutant C116G/C156A encodes two amino acid changes within the C_3HC_4 domain (Fig. 1), and this domain is deleted in CM2/7 (12) (Fig. 1). Based upon the solution structures of the C_3HC_4 zinc fingers from the promyelocytic leukemia proto-oncoprotein (PML) and EHV-63 proteins, the above single amino acid changes within the ICP0 C_3HC_4 domain would be predicted to disrupt one of two Zn^{2+} coordination sites within this domain. Mutagenesis of cysteine-116 and -156 (C116G/C156A) would be predicted to abolish Zn^{2+} coordination (4, 6).

Transient-expression assays. The ability of ICP0 to activate gene expression from a wide range of viral and cellular gene promoters has been used extensively as a measure of its function in mutational analyses (9, 11, 12, 19, 21, 23). Therefore, the ICP0 mutants described in Fig. 1 were screened in transient-expression assays for their ability to activate gene expres-

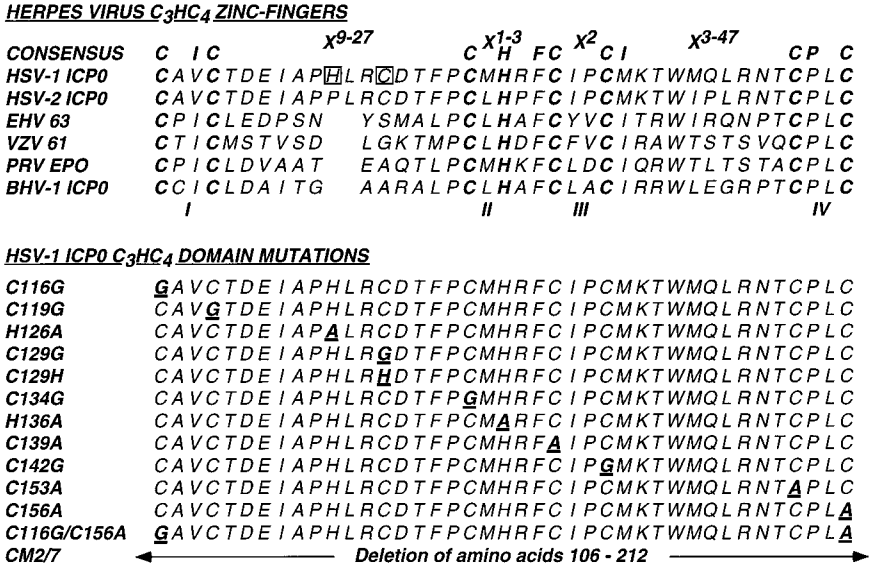

FIG. 1. Consensus herpesvirus C_3HC_4 zinc fingers and the mutations constructed in the HSV-1 ICP0 C_3HC_4 domain. (Top) Alignment of the consensus C_3HC_4 zinc finger amino acid sequence, the HSV-1 ICP0 C_3HC_4 domain (aa 116 to 156), and the related domains of several herpesvirus ICP0 homologs. The conserved cysteines and histidine of these domains are indicated in boldface type, and the pairs of Zn^{2+}-coordinating amino acids are indicated by roman numerals. The nonconsensus cysteine and histidine within the HSV-1 ICP0 C_3HC_4 domain are boxed. (Bottom) Site-directed mutagenesis of the HSV-1 α0 gene was performed to alter each of the cysteine and histidine residues within the consensus ICP0 C_3HC_4 zinc finger into either a glycine or an alanine, as described in Materials and Methods. Cysteine-129 was also changed to a histidine. The mutations are indicated in boldface type and are underlined, and the names of the mutant proteins indicate the amino acid changes and their positions in HSV-1 ICP0.

sion from each of the three major temporal classes (α, β, and γ) of HSV promoters (Fig. 2). This analysis demonstrates that mutagenesis of consensus cysteine (amino acids [aa] 116, 119, 134, 139, 142, 153, and 156) or histidine (aa 136) residues in the C_3HC_4 domain of ICP0, or deletion of this domain (CM2/7), results in the loss of ICP0-mediated transactivation (Fig. 2). Mutagenesis of the nonconsensus histidine in this domain (histidine-126) had no effect on the activity of ICP0 (Fig. 2). In contrast, alteration of cysteine-129, another nonconsensus residue, results in a 60 to 80% reduction in ICP0-mediated transactivation (Fig. 2). Thus, our results demonstrate that the consensus cysteine and histidine residues of the C_3HC_4 domain are required for ICP0-mediated transactivation and suggest that these amino acids constitute a functional C_3HC_4 zinc finger domain (27). They further suggest a role for cysteine-129 in this domain, which is consistent with the conservation of this residue in ICP0 from HSV-1 and HSV-2 (Fig. 1).

Cysteine-129 of HSV-1 ICP0 is not a consensus C_3HC_4 residue and thus would not be predicted to participate in the coordination of Zn^{2+} by this domain. To exclude the possibility that this amino acid participates in the coordination of zinc, we next asked whether histidine, another zinc-coordinating amino acid, could functionally replace cysteine at this position in ICP0. Accordingly, the α0 mutant C129H (Fig. 1) was constructed and screened for its ability to mediate transactivation. Our results demonstrate that replacement of cysteine-129 by a histidine (C129H) abolishes ICP0-mediated transactivation while replacement of this amino acid by glycine (C129G) does not (Fig. 2). These findings argue against a role of cysteine-129 in zinc coordination. Rather, they are consistent with a spatial requirement for cysteine at this position or with a role for this residue in disulfide bonding.

To exclude the possibility that the loss of reporter gene expression resulted from decreased abundance of the mutant forms of ICP0, the accumulation of these proteins in transfected cells was determined by Western blot analysis (Fig. 3). Our findings reveal that their abundance, with the exception of H126A, was increased approximately six- to eightfold relative to that of wild-type ICP0 (Fig. 3). Based on this observation, cotransfection assays were performed to determine whether the increased abundance of the mutant proteins was squelching transcription. This analysis suggests that the loss of reporter gene expression (Fig. 2) did not result from squelching, as the relative levels of ICP0-mediated transactivation did not increase with decreasing amounts of transfected effector plasmids (data not shown). Therefore, the decreased transactivation potential of the ICP0 mutants did not result from alterations in their abundance (Fig. 2 and 3). These data establish a correlation between mutagenesis of the C_3HC_4 domain, the loss of ICP0-mediated transactivation, and an increase in the accumulation of ICP0.

Intranuclear localization of ICP0. In transfected or infected cells, ICP0 is found predominantly in the nucleus, where it colocalizes with, and modifies, ND10 domains (2, 25, 45). The association of ICP0 with ND10s results in the dispersal of ND10-associated proteins (25, 46). Although the relevance of these observations in the context of a productive herpesvirus infection is unknown, the redistribution of ND10-associated proteins may represent a pre- or posttranscriptional event that results in favorable intracellular conditions for HSV gene expression and/or DNA replication (25).

Previous studies have demonstrated that mutations in ICP0 alter its intranuclear localization and its ability to disperse the ND10-associated proteins PML and sp100 (25, 46). These studies indicate that the carboxy terminus of ICP0 (aa 680 to 767) is required for targeting of ICP0 to ND10s and that the C_3HC_4 domain is required for the dispersal of PML and sp100 (25, 46). However, the mutant proteins used in those studies had large deletions in ICP0. Therefore, we asked whether point mutations within the C_3HC_4 domain alter the intracellular localization of ICP0.

Vero cells were transfected with plasmids directing the ex-

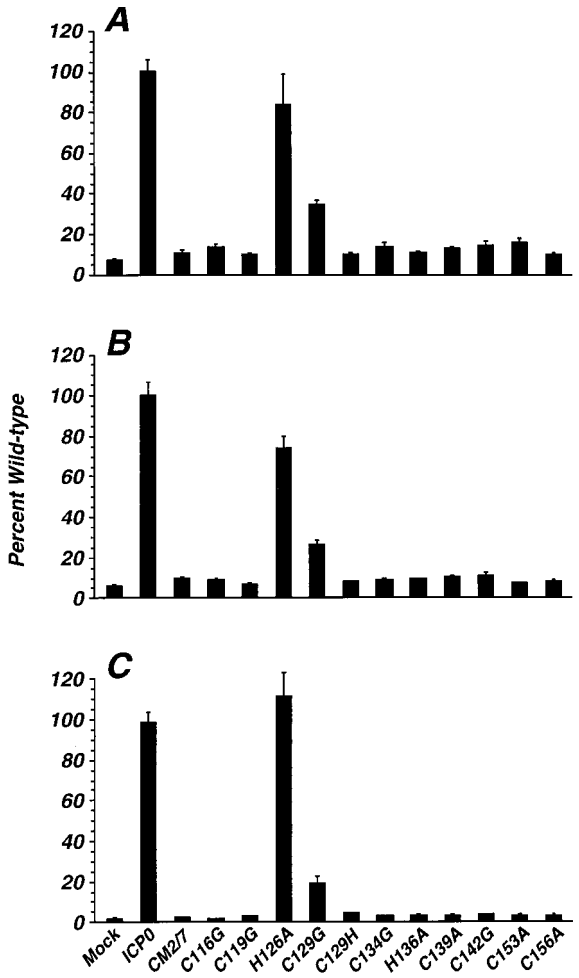

FIG. 2. ICP0-mediated activation of reporter gene expression in cells cotransfected with plasmids directing the expression of wild-type HSV-1 ICP0 or the indicated mutant ICP0 proteins and reporter plasmids encoding the firefly luciferase gene under the control of the ICP4 (A), thymidine kinase (B) or glycoprotein C (C) promoter from HSV-1. Total-cell extracts were prepared at 48 h posttransfection, and luciferase activities were quantified as described in Materials and Methods. Luciferase activities derived from cells expressing the mutant ICP0 proteins are expressed relative to those of cells expressing wild-type ICP0. Cells transfected with reporter plasmids only are indicated (Mock).

pression of wild-type ICP0 or the mutant ICP0 proteins C116G, H126A, C116G/C156A, or CM2/7 (Fig. 1). At 48 h posttransfection, the intracellular distribution of ICP0 was determined by indirect immunofluorescence (Fig. 4). This analysis demonstrates the following. (i) Wild-type ICP0 and H126A localize in highly regular punctate nuclear structures (Fig. 4), a subset of which are defined as ND10 domains (44). (ii) The intranuclear distribution of C116G is highly irregular (Fig. 4), as it was found in both micropunctate and large nuclear granules. (iii) The double mutant C116G/C156A and the deletion mutant CM2/7 are distributed diffusely throughout the nuclei of transfected cells, suggesting that these proteins fail to associate with ND10 domains (Fig. 4).

To address the possibility that the increased abundance of CM2/7, C116G, or C116G/C156A in transfected cells (Fig. 3) altered their intranuclear localization, Vero cells were transfected with 0.5, 2, or 15 μg of plasmid DNAs, and ICP0 was detected by indirect immunofluorescence. The intensity of ICP0 staining in transfected cells increased with the quantity of transfected DNA, yet the intranuclear distribution of ICP0 remained essentially unchanged (data not shown). Thus, the aberrant localization of CM2/7, C116G, and C116G/C156A does not result from their increased abundance. This conclusion is further supported by our observation that the abundance of C116G and C116G/C156A in transfected cells is equivalent (Fig. 3) yet their intranuclear distribution is very different (Fig. 4).

Construction of recombinant herpesviruses. The α0 cDNAs pEL0-C116G, pEL0-H126A, and pEL0-C116G/C156A were introduced into the HSV-1 genome by homologous recombination. The resulting recombinant viruses (vC116G, vH126A, and vC116G/C156A, respectively) direct the expression of the mutant proteins C116G, H126A, and C116G/C156A, respectively (Fig. 1). The predicted sequence arrangements of the α0 genomic loci and the sequences encoding the mutant ICP0 C_3HC_4 domains were verified by Southern blot analysis (Fig. 5) and DNA sequencing (data not shown). The viruses vCPc0 (55), which expresses the α0 cDNA (81), and vCM2/7 (11) have been described previously.

Recombinant virus growth. Growth curves were generated to assess the effects of mutations in the C_3HC_4 domain on the growth of HSV-1 in tissue culture. Vero cells were infected at MOIs of either 0.1 or 10 and harvested at the indicated times postinfection. Virus yields were determined by titration on the ICP0-complementing cell line L7. Our findings demonstrate that in high-multiplicity infections, mutagenesis of the ICP0 C_3HC_4 domain has only a small effect on the growth rates and yields of the mutant viruses relative to vCPc0, the parent cDNA virus. The α0 mutant viruses vCM2/7, vC116G, vH126A, and vC116G/C156A and the α0 deletion virus *dl*1403 exhibited a slight delay in growth kinetics at early times postinfection (Fig. 6B), yet their yields were similar to those of vCPc0 or wild-type HSV-1 at 24 h postinfection (Fig. 6B). In low-multiplicity infections, viruses with deleterious mutations in the C_3HC_4 domain (vCM2/7, vC116G, and vC116G/C156A) exhibited growth kinetics and yields similar to those of the α0 deletion virus *dl*1403 (Fig. 6A). However, at very late times postinfection (48 to 72 h), these mutants yielded wild-type levels of virus (Fig. 6A). This result is consistent with the multiplicity-dependent growth of α0 mutant viruses.

Previous studies reveal that mutagenesis, or deletion, of the α0 gene from HSV-1 results in high particle/PFU ratios (10, 11, 70). Here, analyses were performed to determine the relative genome/PFU (10) and particle/PFU ratios for wild-type HSV-1, vCPc0, vCM2/7, vC116G, vH126A, vC116G/C156A, and *dl*1403. The genome/PFU ratios of these viruses were determined by comparison of the levels of DNA hybridization

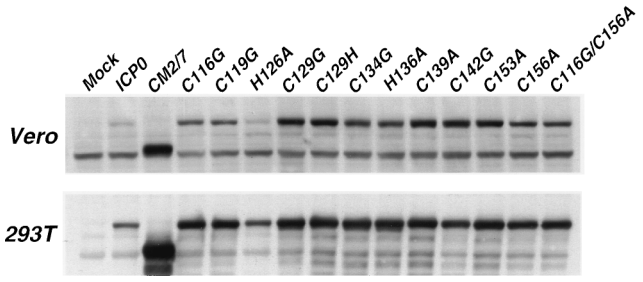

FIG. 3. Western blot analysis of the abundance of ICP0 in transfected cells. Vero or 293T cells were either mock transfected (Mock) or transfected with plasmids directing the expression of wild-type ICP0 or the indicated mutant ICP0 proteins. Cell extracts were prepared at 48 h posttransfection, and the relative abundance of ICP0 was determined by Western blot analysis, using the rabbit polyclonal antibody CLU7 (anti-ICP0), as described in Materials and Methods.

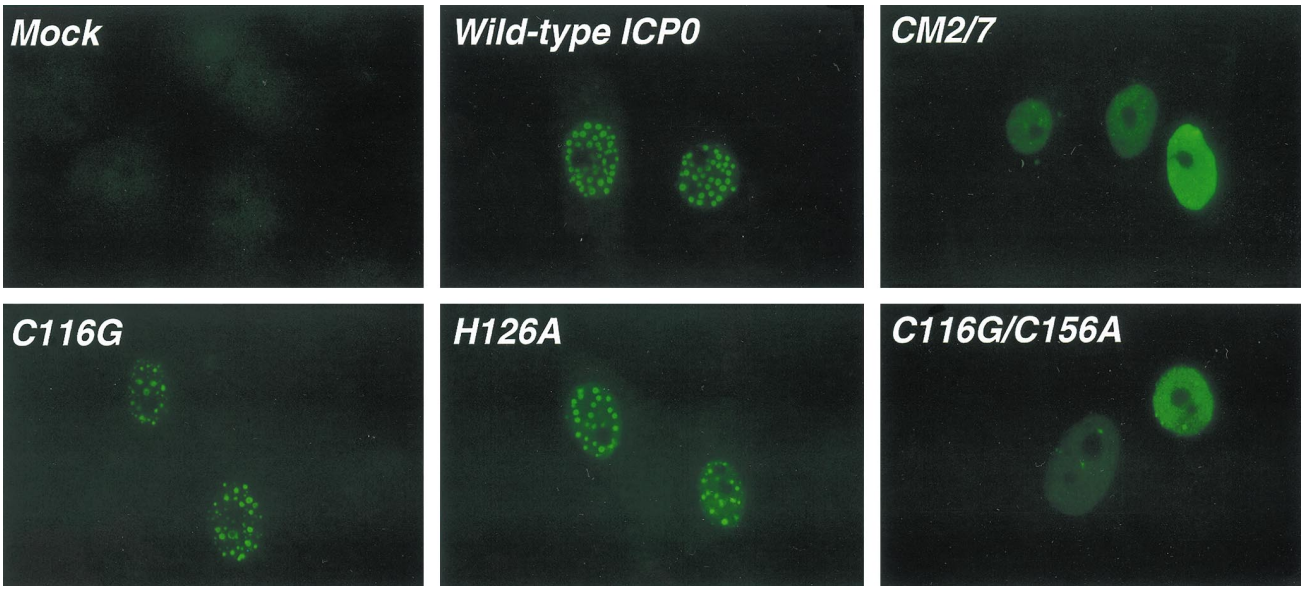

FIG. 4. Intracellular localization of ICP0. Vero cells were either mock transfected or transfected with plasmids directing the expression of wild-type ICP0 or the indicated mutant ICP0 proteins. At 48 h posttransfection, the cells were fixed and reacted with the rabbit polyclonal antibody CLU7 (anti-ICP0) followed by fluorescein isothiocyanate-conjugated secondary antibodies. Representative fields of cells were photographed using a Leitz Dialux microscope with optical systems for the selective visualization of fluorescein and the Nikon UFX-DXII photographic system.

from samples prepared at 1 h postinfection to the titer of each virus stock as assayed on L7 cells (see Fig. 8). Our analyses demonstrate that all viruses tested, with the exception of *dl*1403, exhibit wild-type genome/PFU ratios (see Fig. 8). The particle/PFU ratios of wild-type HSV-1, vC116G, vH126A, and vC116G/C156A were also determined, as described in Materials and Methods, and confirm the genome/PFU ratios. Therefore, all viruses tested, with the exception of *dl*1403, exhibit wild-type genome/PFU ratios (see Fig. 8). This finding was dependent upon titration of these viruses on the complementing cell line L7, as titration of these viruses on the complementing cell line 0-28 (63) or U2OS (80) consistently underrepresented their titers by 30- to 100-fold (data not shown). Thus, mutations in the C_3HC_4 domain that abolish ICP0-mediated transactivation alter the intranuclear localization and accumulation of ICP0, and impair the growth and replication of HSV-1 at low MOIs do not alter the particle/PFU ratios of recombinant herpesviruses (see Fig. 8).

These analyses demonstrate that the C_3HC_4 domain is required to achieve wild-type virus growth kinetics in low-multiplicity infections. They further establish a correlation between the ability of ICP0 to mediate transactivation (Fig. 2) and virus growth (Fig. 6).

Virus spread in tissue culture. Indirect immunofluorescence was used to examine the effect of disrupting the ICP0 C_3HC_4 domain on the progression of virus infections at low multiplicities. This analysis demonstrated the following. (i) At 8 h postinfection, ICP0 was localized predominantly in the nuclei of infected cells (Fig. 7). The number of positively staining cells in each infected-cell monolayer and the intensities of ICP0 staining were equivalent for all viruses tested (data not shown). (ii) At 12 h postinfection, wild-type HSV-1 and vH126A had initiated secondary infections, as demonstrated by the formation of syncytia and foci of infected cells. In contrast, in monolayers infected with vC116G or vC116G/C156A, ICP0 was restricted to single cells (Fig. 7). (iii) At 16 h postinfection, wild-type HSV-1 and vH126A were spreading (Fig. 7). However, vC116G and vC116G/C156A only occasionally initiated productive infections, as indicated by the rare formation of foci of infected cells (Fig. 7). (iv) At 24 h postinfection, all of the cells in the monolayers infected with wild-type HSV-1 or vH126A contained virus, as indicated by the presence of ICP0 (Fig. 7). However, in monolayers infected with vC116G or vC116G/C156A, ICP0 was found predominantly in single cells and rarely spread (Fig. 7). Thus, unlike wild-type HSV-1 or

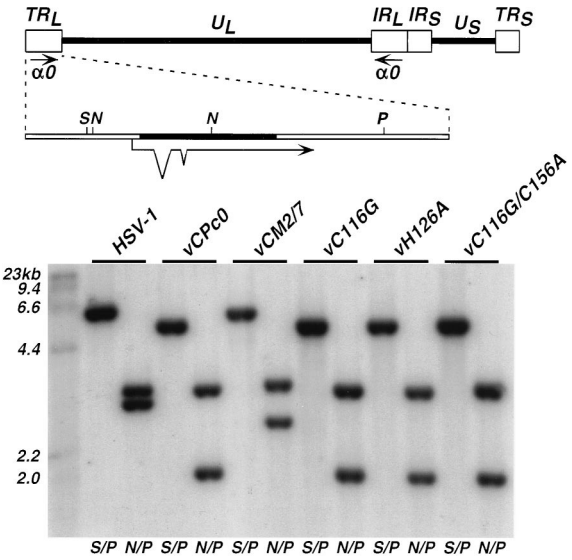

FIG. 5. Southern blot analysis of wild-type and recombinant virus DNAs. Infected-cell DNAs were digested with *Sac*I (S) and *Pst*I (P) or *Not*I (N) and *Pst*I, electrophoretically separated in agarose gels, and transferred to nylon membranes. The blots were hybridized with a randomly primed α0 probe (−810 to +4382), as described in Materials and Methods. The α0 loci of wild-type HSV-1 and vCM2/7 contain two introns (IVS-1 and IVS-2); these loci in the α0 cDNA viruses vCPc0, vC116G, vH126A, and vC116G/C156A lack both IVS-1 and IVS-2.

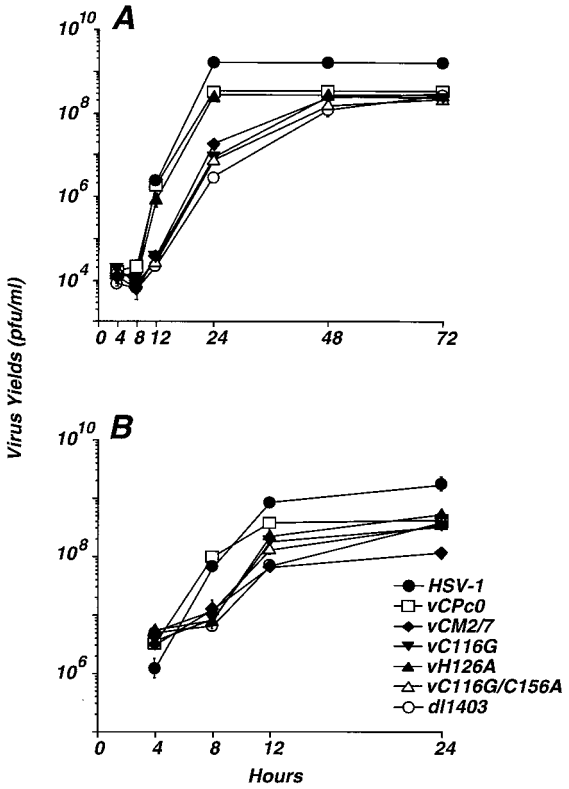

FIG. 6. Growth of wild-type HSV-1 or α0 mutant viruses. The titers of all viruses were determined on L7 cell monolayers prior to growth analyses. Vero cells were infected with wild-type HSV-1, vCPc0, vCM2/7, vC116G, vH126A, vC116G/C156A, or the α0 deletion virus *dl*1403, with either 0.1 (A) or 10 (B) PFU per cell, and the infections were stopped at the indicated times postinfection. The resulting virus yields were titrated on L7 cell monolayers. Growth curves represent the average of three independent infections, each with the titer determined in duplicate.

vH126A, vC116G and vC116G/C156A rarely established productive infections in tissue culture at low multiplicities. Therefore, in the absence of functional ICP0, the probability of establishing a lytic herpesvirus infection at low MOIs is significantly decreased.

DNA replication. Having shown that mutations in the C_3HC_4 domain impair the growth of HSV-1, we sought to determine the basis for this defect. Therefore, we examined virus DNA replication in cells infected with the C_3HC_4 mutant viruses. Vero cells were infected at a MOI of either 0.1 or 10, and total infected-cell DNAs were prepared at 1 and 16 h postinfection. The accumulation of virus DNAs was determined by DNA hybridization with a probe complementary to the HSV-1 α4 gene. In high-multiplicity infections, all viruses with the exception of *dl*1403 exhibited similar levels of DNA replication at 16 h postinfection (Fig. 8). In contrast, at low MOIs, the recombinant viruses vCM2/7, vC116G, and vC116G/C156A exhibited a 12-fold reduction in DNA replication relative to vH126A, vCPc0, or wild-type HSV-1 (Fig. 8). These data imply that the defect in the replication cycle of vCM2/7, vC116G, and vC116G/C156A occurs prior to the initiation of DNA synthesis.

Accumulation of virus-specified proteins. To further characterize the growth and replication defects of viruses with mutations in the ICP0 C_3HC_4 domain, the abundance of representative proteins from each of the three major kinetic classes of virus genes was determined by Western blot analysis. Vero cells were infected at a multiplicity of 0.1 (data not shown), 1, or 10, and cell extracts were prepared at the indicated times postinfection. Infected-cell proteins were detected by using antibodies that recognize the IE proteins ICP0, ICP4, and ICP27, the early protein glycoprotein B (gB), and the late proteins alpha-*trans*-inducing factor (α-TIF) and virion protein 5 (VP5) (Fig. 9). We note that the subtle difference in the mobilities of ICP0 from HSV-1 strain 17 and the recombinant viruses represents strain variations between the α0 gene from HSV-1 strain 17 and the α0 cDNA (81). This analysis demonstrates that in high-multiplicity infections (MOI = 10), all viruses tested with the exception of *dl*1403 accumulated nearly wild-type levels of these proteins (Fig. 9A). However, in low-multiplicity infections (MOI = 0.1 [data not shown] or 1), vCM2/7, vC116G, and vC116G/C156A accumulated low levels of ICP27, gB, α-TIF, and VP5, while the abundances of ICP0 and ICP4 were unaffected (Fig. 9B). Thus, mutations in the C_3HC_4 domain result in significant defects in the accumulation of virus-specified proteins at low MOIs.

Further analysis of the abundance of virus-specified proteins in cells infected with the α0 deletion virus *dl*1403 reveals that this virus accumulated increased levels of the IE protein ICP4 relative to wild-type HSV-1 (Fig. 9B). This increase is a reflection of the higher particle/PFU ratio of *dl*1403 (11, 70). However, the abundance of the IE protein ICP27 was significantly decreased in cells infected with *dl*1403 (Fig. 9B). This observation clearly implies inherent differences between the regulation of the expression and/or synthesis of ICP4 and ICP27 at early times of infection.

Based on the growth and replication of vCM2/7, vC116G, vC116G/C156A, and *dl*1403 (Fig. 6 to 8), decreases in the abundance of early and late virus proteins in cells infected with these mutants were expected (Fig. 9). However, a decrease in the abundance of the essential IE protein ICP27 was unexpected, as IE gene transcription is independent of de novo protein synthesis (Fig. 9) (13, 38, 71). Previous studies demonstrated that ICP27 is required for the expression of HSV early and late genes in productive infections (65, 67, 73). Therefore, significant decreases in the accumulation of ICP27 would be predicted to result in defects in the accumulation of early and late virus proteins and in virus growth. These observations support our conclusion that ICP0 regulates the expression of ICP27 and that the multiplicity-dependent growth of α0 mutant viruses is due, in part, to low levels of ICP27.

Previous studies have demonstrated that ICP0 is difficult to extract from infected cells (1, 34). Thus, to control for the recovery of ICP0, experiments were performed to address the solubility of wild-type and mutant forms of this protein in infected cells by using an extraction method developed to enhance the recovery of virus proteins (see Materials and Methods) (Fig. 10). This analysis reveals that all viruses tested, with the exception of *dl*1403, accumulated nearly identical levels of soluble ICP0 and ICP27 (Fig. 10A). However, the relative abundance of insoluble ICP0 was increased in cells infected with vC116G or vC116G/C156A (Fig. 10B). Thus, point mutations in the C_3HC_4 domain appear to decrease the solubility of ICP0. We further noted that the mutant ICP0 protein CM2/7 did not partition with the insoluble fraction (Fig. 10B). It is interesting that substitution mutations within the C_3HC_4 domain reduced the solubility of ICP0 while deletion of this domain appeared to cause the opposite effect.

To exclude the possibility that the altered solubility of the mutant proteins was a general property in cells infected with vCM2/7, vC116G, or vC116G/C156A, the solubility of ICP27 was also examined. Unlike ICP0, ICP27 is highly soluble (Fig. 10). This analysis further demonstrates that at low MOIs the

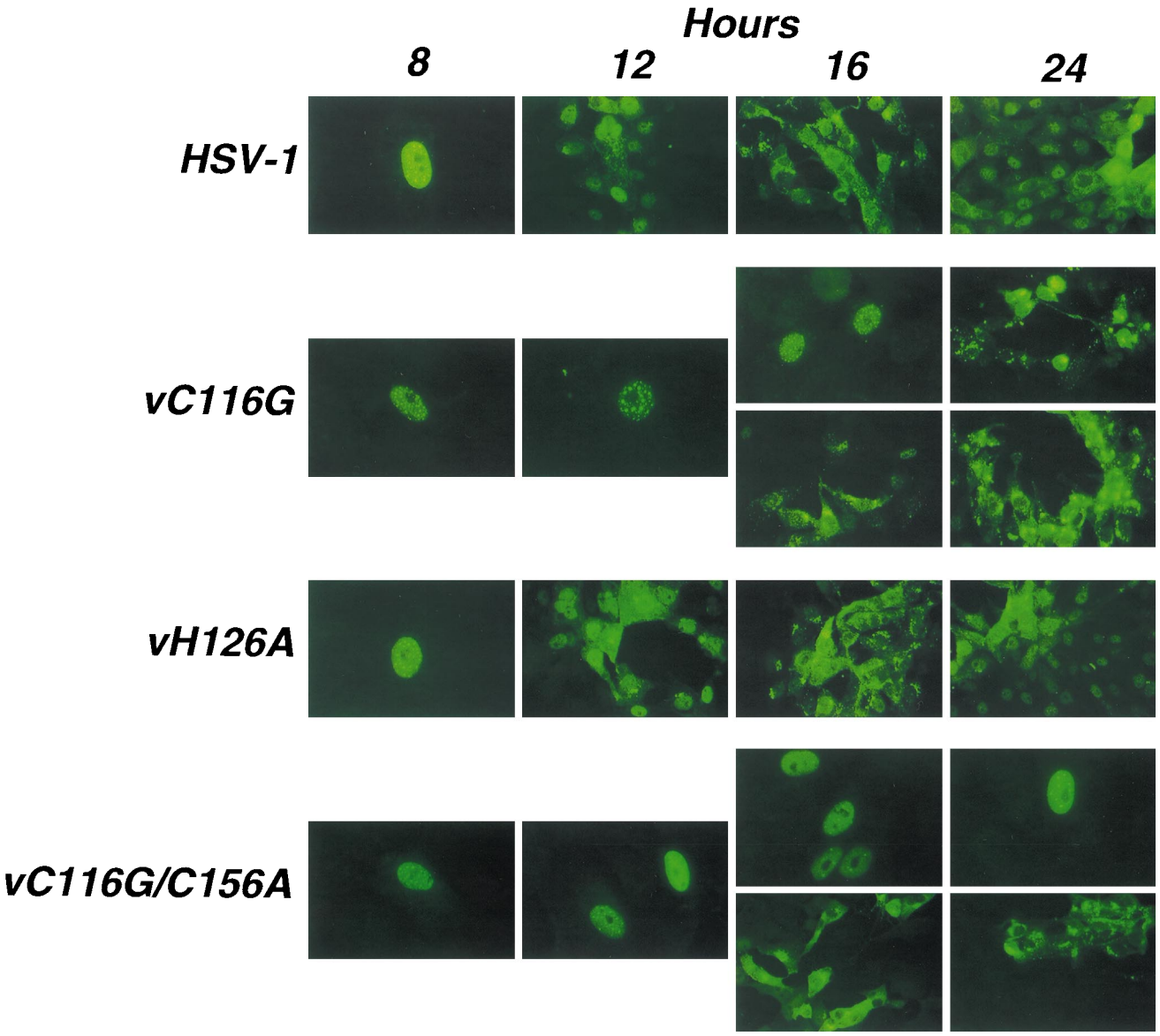

FIG. 7. Analysis of HSV-1 infections by indirect immunofluorescence. Vero cells were infected with the indicated viruses at a MOI of 0.01. At the indicated times postinfection, the cells were fixed and reacted with the rabbit polyclonal antibody CLU7 (anti-ICP0) followed by FITC-conjugated secondary antibodies. Representative fields of cells were photographed by using a Leitz Dialux microscope with optical systems for the selective visualization of fluorescein and the Nikon UFX-DXII photographic system. At 16 and 24 h postinfection, two fields of cells infected with vC116G or vC116G/C156A are shown to indicate the restricted growth of these viruses and their rare spread.

abundance of ICP27 in cells infected with vCM2/7, vC116G, or vC116G/C156A was reduced 12-fold relative to that of wild-type HSV-1 or vH126A (Fig. 10).

Synthesis of IE proteins. Having shown that mutations in the α0 gene, which result in a loss of function (Fig. 2), also result in defects in the accumulation of ICP27 in low-multiplicity infections, we performed experiments to examine the synthesis of IE proteins at early and late times postinfection. Vero cells were infected at a MOI of 0.5 with wild-type HSV-1 or the mutant viruses and pulse-labeled for 30 min with ^{35}S at 3.5 and 8 h postinfection (as described in Materials and Methods). ICP0, ICP4, and ICP27 were quantitatively immunoprecipitated and separated by SDS-PAGE (Fig. 11). At 3.5 h postinfection, all of the viruses tested, except *dl*1403, synthesized nearly equivalent amounts of ICP0 and ICP4 (Fig. 11). However, in cells infected with vCM2/7, vC116G, vC116G/C156A, or *dl*1403, the synthesis of ICP27, relative to ICP4, was reduced (Fig. 11; Table 1). At 8 h postinfection, these mutants exhibited significant reductions in the synthesis of ICP0, ICP4, and ICP27 relative to wild-type HSV-1, vCPc0, or vH126A (Fig. 11). These data further support the notion that ICP0 regulates the expression and/or synthesis of ICP27 at early times postinfection and that ICP0 may regulate the expression of other IE gene products at late times.

Stability of ICP0. Based on the observation that the accumulation of mutant forms of ICP0 in cells infected with vCM2/7, vC116G, or vC116G/C156A is nearly wild type (Fig. 9) despite significant reductions in the synthesis of ICP0 (Fig. 11), we predicted that these mutations increase the stability of ICP0. Therefore, pulse-chase experiments were performed to

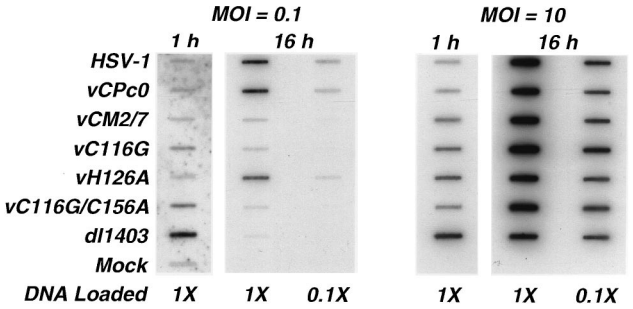

FIG. 8. DNA replication of wild-type and mutant viruses. Vero cells were either mock infected (Mock) or infected with wild-type HSV-1, vCPc0, vCM2/7, vC116G, vH126A, vC116G/C156A, or the α0 deletion virus *dl*1403, at either low (MOI = 0.1) or high (MOI = 10) MOIs. Total infected-cell DNAs were prepared at 1 and 16 h postinfection, and 10-fold dilutions (0.1×) of DNAs were slot blotted to nylon membranes. The infected-cell DNAs were hybridized with a probe complementary to the HSV-1 α4 loci, and the relative abundance of virus genomes was determined by PhosphorImager analysis using ImageQuaNT software, as described in Materials and Methods. Note that prior to these analyses, all virus titers were determined on the ICP0-expressing cell line L7.

determine the $t_{1/2}$ of wild-type and mutant forms of ICP0. Vero cells were infected at a MOI of 0.5, pulse-labeled with ^{35}S for 30 min at 2.5 h postinfection, and either harvested immediately or chased for 2 or 4 h (as described in Materials and Methods). ICP0, ICP4, and ICP27 were quantitatively immunoprecipitated and analyzed by SDS-PAGE (Fig. 12; ICP27 not shown). This analysis demonstrates that the stability of CM2/7 and C116G/C156A was increased approximately 2.5-fold relative to that of wild-type ICP0. The $t_{1/2}$ of wild-type ICP0 was approximately 1.5 h, whereas the $t_{1/2}$ of these ICP0 mutants appeared to be greater than 3 h. The stability of ICP4 (Fig. 12B) and ICP27 (data not shown) was not affected by these alterations in ICP0. These findings explain the above discrepancy between the synthesis of ICP0 (Fig. 11) and its accumulation (Fig. 9).

Synthesis of ICP0, ICP4, and ICP27 at early times of infection. Elshiekh et al. (17) demonstrated that synthesis of ICP0 precedes, and is important for, the maximal accumulation of IE mRNAs. We show in Fig. 11 that the synthesis of ICP27 in cells infected with vCM2/7, vC116G, vC116G/C156A or *dl*1403 is decreased at early times postinfection. Therefore, IE protein synthesis was examined at very early times postinfection to ascertain the order of expression of ICP0, ICP4, and ICP27. Vero cells were infected at a MOI of 0.5 and pulse-labeled for 30 min at the indicated times, as above. ICP0, ICP4, and ICP27 were quantitatively immunoprecipitated and analyzed, as described in Materials and Methods. This analysis demonstrates that α0 mutant viruses synthesized low levels of ICP27, relative to wild-type HSV-1, at early times postinfection (Fig. 13). They further reveal that the synthesis of ICP0, ICP4, and ICP27 proceeds in an ordered cascade, with the synthesis of ICP0 preceding that of ICP4 and ICP27 (Fig. 13). Thus, these findings support a role for ICP0 in the synthesis of ICP27 at early times postinfection.

Accumulation of α0, α4, and α27 RNAs. Mutagenesis of consensus C_3HC_4 residues within ICP0, or deletion of the α0 gene, leads to significant reductions in the synthesis of the essential immediate-early protein ICP27 in infected cells. Therefore, the abundance of α27 RNA in low-multiplicity infections was examined. Vero cells were infected at a MOI of 0.5, and total RNAs were extracted at 2, 4, and 7 h postinfection. The relative abundance of the α0, α4, and α27 RNAs was determined by RT-PCR under conditions where amplification of target sequences was linear and no amplification occurred in the absence of RT. The accumulation of IE RNAs at 2 h postinfection was not altered in cells infected with any of the viruses tested (Fig. 14). However, at 4 h postinfection in cells infected with vC116G/C156A or *dl*1403, the abundance of α27 RNA was reduced fourfold (Fig. 14) while the abundance of α0 RNA in cells infected with vC116G/C156A was reduced twofold. No significant reduction in the abundance of α4 RNA was observed. At 7 h postinfection, the abundance of IE RNAs in cells infected with these mutants was reduced 4- to 10-fold relative to that in cells infected with the parent cDNA virus vCPc0 (Fig. 14). Thus, ICP0 augments the accumulation of its own RNA and is required for the accumulation of wild-type levels of α27 RNA. We further note that in contrast to high-multiplicity infections (17), the IE RNAs examined continued to accumulate at late times in low-multiplicity infections and that this accumulation appears to be dependent on the pres-

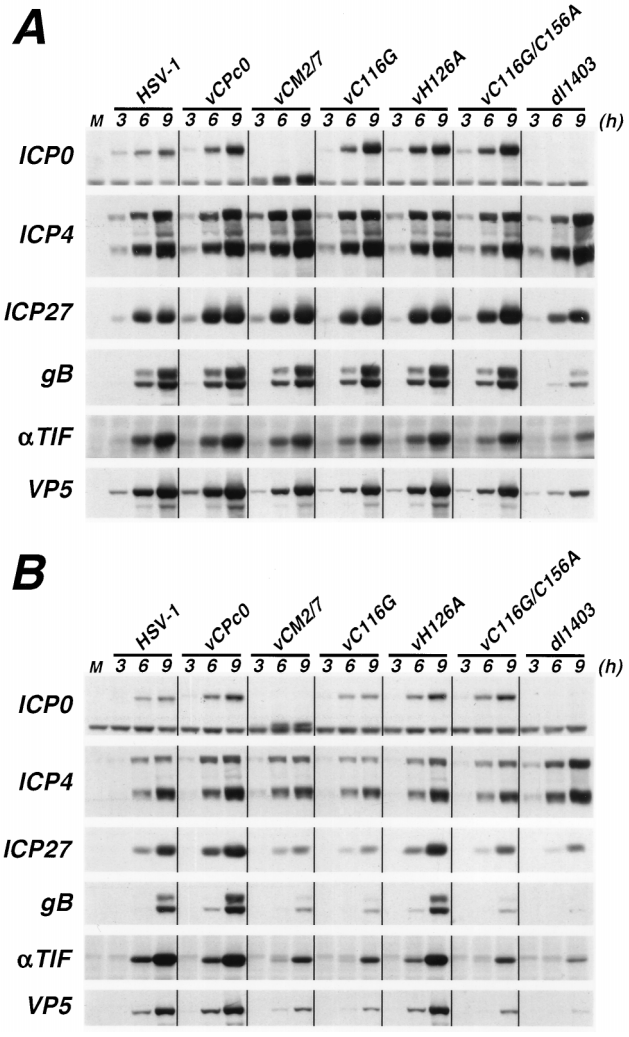

FIG. 9. Accumulation of virus-specified proteins in infected cells. Vero cells were infected with the indicated viruses at a MOI of either 10 (A) or 1 (B), and infected-cell extracts were prepared at the indicated times. The relative abundance of the indicated HSV proteins was determined by Western blot analysis using the mouse monoclonal antibody 58S (anti-ICP4) or the rabbit polyclonal antibody CLU7 (anti-ICP0), CLU38 (anti-ICP27), R69 (anti-gB), anti-αTIF, or NC-1 (anti-VP5). Secondary antibodies were conjugated to horseradish peroxidase, and immunoblots were developed with the chemiluminescent substrate LumiGLO. The abundance of the indicated HSV proteins was quantified, as described in Materials and Methods.

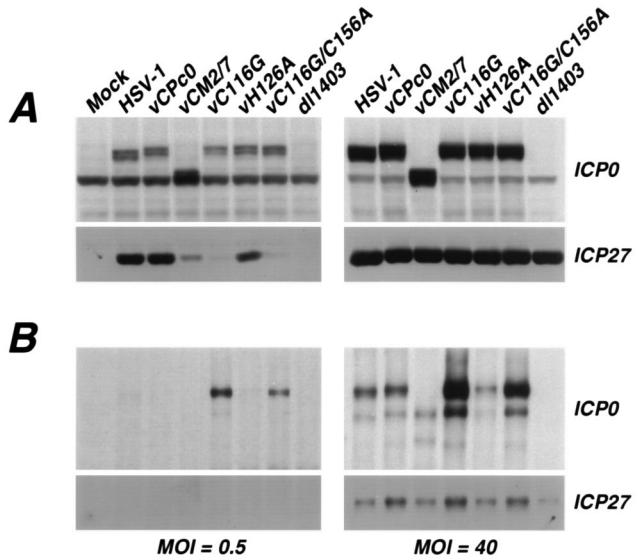

FIG. 10. Solubility of ICP0 in cells infected with wild-type HSV-1 or α0 mutant viruses. Vero cells were infected with the indicated viruses at either low (MOI = 0.5) or high (MOI = 40) MOIs, as indicated. At 8 h postinfection, infected-cell lysates were prepared, as described in Materials and Methods, and the soluble (A) and insoluble (B) protein fractions were separated by centrifugation. The relative abundance of the indicated proteins was determined by Western blot analysis using the rabbit polyclonal antibodies CLU7 (anti-ICP0) and CLU38 (anti-ICP27). Secondary antibodies were conjugated to horseradish peroxidase, and immunoblots were developed with the chemiluminescent substrate LumiGLO. The abundance of the indicated HSV proteins was quantified, as described in Materials and Methods.

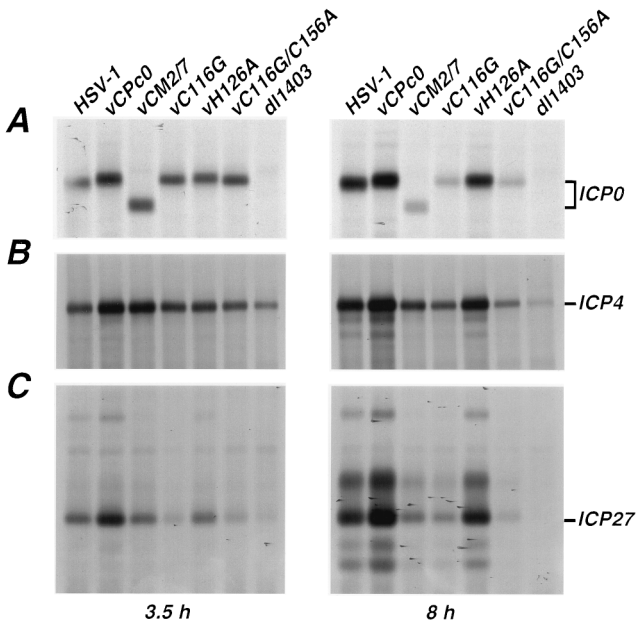

FIG. 11. Synthesis of IE proteins. Vero cells were infected with the indicated viruses at a MOI of 0.5 and labeled for 30 min at 3.5 h (left) and 8 h (right) postinfection with 200 μCi of Tran^{35}S Label in 500 μl of Met-free DMEM. Infected-cell lysates were prepared, and ICP0 (A), ICP4 (B), or ICP27 (C) was quantitatively immunoprecipitated with monoclonal antibody 1114 (anti-ICP4) or the rabbit polyclonal antibody CLU7 (anti-ICP0) or CLU38 (anti-ICP27). The immunoprecipitated proteins were separated by SDS-PAGE and visualized by fluorography. The synthesis of ICP27 was quantified relative to that of ICP4, as described in Materials and Methods.

ence of functional ICP0 (Fig. 14). Thus, at late times postinfection, ICP0 affected the accumulation of IE RNAs.

DISCUSSION

This study examined the role of the consensus C_3HC_4 zinc finger of ICP0 in the growth and replication of HSV-1. Mutations in the α0 gene were constructed to alter each of the cysteine and histidine residues within this domain, and the effects of these mutations on ICP0 function were examined in transient-expression assays and in the context of a productive HSV infection. We conclude that alteration of the consensus C_3HC_4 residues abolishes ICP0-mediated transactivation, alters the intranuclear distribution of ICP0, and results in a significant increase in its stability. We further show that these mutations, in the context of the virus genome, result in profound defects in the growth and replication of HSV-1 in low-multiplicity infections. Our findings reveal a role for ICP0 in the expression of the essential IE gene α27 and support the conclusion that the multiplicity-dependent growth of α0 mutant viruses may result from reduced levels of ICP27.

The primary amino acid sequence of ICP0 results in the classification of ICP0 as a member of the C_3HC_4 zinc finger (RING) family of proteins (27, 28). Previous studies have demonstrated a role for members of this family in transcription, differentiation, oncogenesis, DNA repair, and recombination (references 27 and references therein). Here, we report that alterations of the C_3HC_4 residues of ICP0 reveal that they are required for the activation of reporter genes in transient-expression assays. Moreover, the failure of mutants containing these alterations to activate reporter gene expression did not result from changes in their abundance (Fig. 3). These findings are consistent with those from previous studies, although the cysteine and histidine residues were not examined in those analyses (12, 18, 21, 68).

ICP0 localizes predominantly to the nucleus of transfected or infected cells (1, 30, 56, 78), where it associates with and modifies ND10 domains (25). The ICP0 C_3HC_4 domain is required for the dispersal of ND10-associated proteins (25, 45, 46). We have demonstrated that alterations in the putative zinc-coordinating residues of this domain disrupt the intranuclear localization of ICP0. Thus, we conclude that the C_3HC_4 domain is important for the intranuclear distribution of ICP0 and its localization to ND10s.

Our finding that the C_3HC_4 domain plays a role in the intranuclear localization of ICP0 is in contrast to that of Everett and Maul (25), who have implicated the carboxy-terminal 180 aa of ICP0 in its targeting to ND10s. However, our findings are consistent with those of Borden et al. (6), who demonstrate that alteration of the consensus C_3HC_4 cysteines of PML results in the loss of PML localization to ND10 domains. These

TABLE 1. Densitometric analysis of the synthesis of ICP27 relative to ICP4 at 3.5 h postinfection

Protein	Density of[a]:						
	HSV-1	vCPc0	vCM2/7	vC116G	vH126A	vC116G/C156A	dl1403
ICP4	137	183	174	136	136	129	89
ICP27	116	171	109	60	101	68	52
ICP27/ICP4 ratio	0.85	0.93	0.63	0.44	0.74	0.56	0.58

[a] The numbers are pixel densities from scanned films.

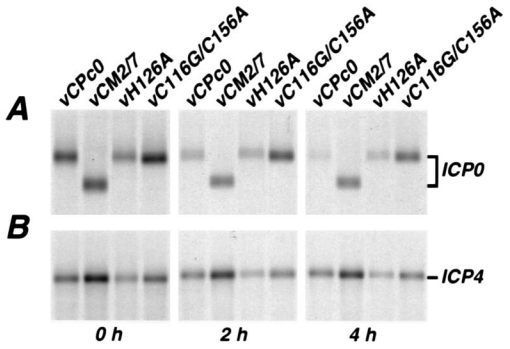

FIG. 12. Stability of ICP0 in infected cells. Vero cells were infected with the indicated viruses at a MOI of 0.5 and labeled for 30 min at 2.5 h postinfection with 200 μCi of Tran^{35}S Label in 500 μl of Met-free DMEM. At 3 h postinfection, the cell monolayers were rinsed twice with growth medium to remove the free label, and the label was chased for 0, 2, or 4 h at 37°C, as indicated. Infected-cell lysates were prepared, and ICP0 (A) and ICP4 (B) were quantitatively immunoprecipitated with the rabbit polyclonal antibody CLU7 (anti-ICP0) or the monoclonal antibody 1114 (anti-ICP4), respectively. Immunoprecipitated ICP0 and ICP4 were separated by SDS-PAGE and analyzed by fluorography. Densitometric analysis was performed as described in Materials and Methods.

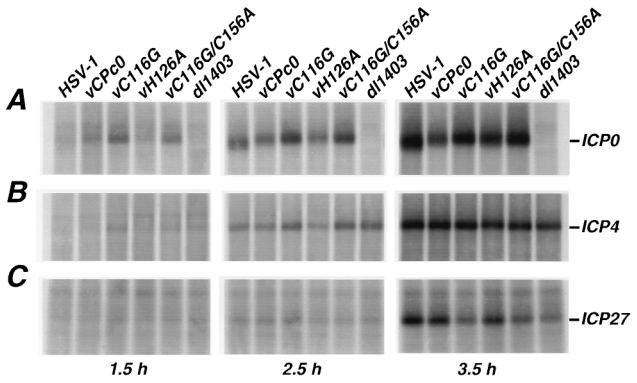

FIG. 13. Synthesis of IE proteins at very early times postinfection. Vero cells were infected with the indicated viruses at a MOI of 0.5 and labeled for 30 min at 1.5, 2.5, or 3.5 h postinfection with 200 μCi of Tran^{35}S Label in 500 μl of Met-free DMEM. Infected-cell lysates were subsequently prepared at 2, 3, and 4 h postinfection. ICP0 (A), ICP4 (B), and ICP27 (C) were quantitatively immunoprecipitated with monoclonal antibody 1114 (anti-ICP4) or the rabbit polyclonal antibody CLU7 (anti-ICP0) or CLU38 (anti-ICP27), respectively. Immunoprecipitated ICP0, ICP4, and ICP27 were separated by SDS-PAGE and analyzed by fluorography. Protein synthesis was quantified by densitometric analysis, as described in Materials and Methods.

data may be reconciled by a requirement for the participation of both the C_3HC_4 domain and the carboxy terminus in the efficient localization of ICP0 to ND10 domains. This conclusion is consistent with the inability of the carboxy terminus of ICP0 to direct a fusion protein between this domain and β-galactosidase to ND10 domains (25).

The critical role of ICP0 in the growth and replication of HSV-1 in low-multiplicity infections was revealed by analysis of the growth kinetics of α0 mutant viruses. Viruses with deleterious mutations in the α0 gene (vCM2/7, vC116G, vC116G/C156A, and *dl*1403) exhibited severely delayed growth kinetics and reduced yields at low MOIs (Fig. 6) (9, 12, 20, 70). However, at high MOIs, these viruses exhibited nearly wild-type growth kinetics and yields (Fig. 6). The basis for this MOI-dependent growth was examined by comparing the development of infected-cell foci in Vero cell monolayers infected with vC116G, vC116G/C156A, vH126A, or wild-type HSV-1 by using indirect immunofluorescence (Fig. 7). This analysis demonstrated that, in contrast to wild-type HSV-1 and vH126A, vC116G and vC116G/C156A rarely formed foci of infected cells (Fig. 7). In the rare instances when vC116G or vC116G/C156A completed the HSV reproductive cycle, secondary infections in the adjacent cells were initiated at high MOIs. This observation explains the nearly wild-type yields of these viruses at 48 to 72 h postinfection (Fig. 6). Our results demonstrate that viruses with deleterious mutations in the α0 gene complete the lytic life cycle in approximately 1% of infected cells. The failure of vC116G and vC116G/C156A to efficiently initiate productive infections at low MOIs supports the conclusion that the rare formation of infected-cell foci results from partial complementation of IE events by a cell cycle-dependent function (8).

To identify the point during the HSV life cycle at which ICP0 is required to achieve wild-type virus growth and replication, we examined virus-specified macromolecular synthesis in low- and high-multiplicity infections. These analyses demonstrate that viruses with deleterious mutations in the α0 gene accumulate decreased levels of virus DNA in cells infected at low but not high MOIs (Fig. 8). A kinetic analysis of the abundance of virus-specified proteins at low MOIs revealed a defect in the accumulation of the essential IE protein ICP27 and of early and late proteins (Fig. 9). This observation is consistent with the essential role of ICP27 in the expression of early and late virus-specified gene products (47, 62, 65, 67, 73). Analysis of the synthesis of IE proteins at early and late times postinfection led us to conclude that deleterious mutations in the α0 gene result in significant decreases in the synthesis of ICP27 at early times postinfection and of ICP0, ICP4, and ICP27 at late times postinfection.

Analysis of mutant forms of ICP0 in infected cells revealed a discrepancy between the synthesis and the abundance of these proteins (Fig. 9 and 11). To resolve this discrepancy, the stability of ICP0 in cells infected with vCM2/7, vC116G/C156A, vH126A, or vCPc0, relative to that of ICP4, was ex-

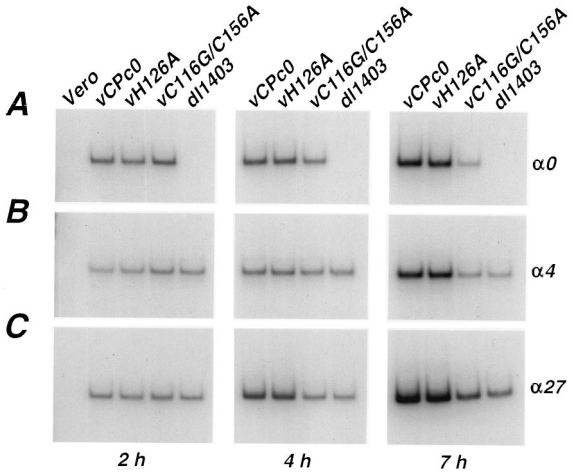

FIG. 14. Accumulation of HSV IE RNAs in infected cells. Vero cells were infected with the indicated viruses at a MOI of 0.5, and total-cell RNAs were prepared at 2, 4, and 7 h postinfection. The indicated IE RNAs (α0, α4, and α27) were amplified by RT-PCR in the presence of [γ-^{32}P]dCTP under linear amplification conditions, as described in Materials and Methods. The amplification products were separated by electrophoresis through polyacrylamide gels and visualized by autoradiography. Control RT-PCR amplifications were performed to demonstrate the linearity of these reactions and the absence of contaminating DNA (see Materials and Methods).

amined in a pulse-chase experiment. This analysis demonstrates that the half-lives of CM2/7 and C116G/C156A were increased approximately 2.5-fold relative to that of wild-type ICP0.

Classification as an HSV IE gene requires transcription in the absence of de novo protein synthesis (13, 37, 38, 71). In these studies, we identify a hierarchy of expression within the class of IE proteins. This hierarchy is revealed by our studies of protein synthesis at very early times postinfection. We demonstrate that the order of appearance of nascent ICP0, ICP4, and ICP27 begins with ICP0, which is followed by ICP4 and finally ICP27 (Fig. 13). This finding is consistent with our hypothesis that ICP0 regulates the synthesis of ICP27 at these times postinfection. While IE RNAs accumulated to similar levels in cells infected with mutant or wild-type viruses at 2 h postinfection (Fig. 14), the synthesis of ICP27 was not detected at this time (Fig. 13). In contrast, synthesis of ICP0 and, to a lesser extent, ICP4 was detected. This discordance between the presence of α27 RNA and the absence of protein reinforces our hypothesis that ICP0 regulates the production of ICP27. This hypothesis is consistent with the observation that ICP0 interacts with EF-1δ, a major translational regulatory factor (39).

The experiments we have described also demonstrate that deleterious mutations in ICP0 affect the accumulation of IE RNAs at late times postinfection. Thus, the synthesis of ICP0 with alterations in, or deletions of, the C_3HC_4 domain results in decreased accumulation of all IE RNAs examined at 7 h postinfection.

In conclusion, we have provided evidence that ICP0 plays a central role in the regulation of expression of HSV IE proteins throughout the lytic cycle.

ACKNOWLEDGMENTS

This study was supported by Public Health Service grant AI-33952 to Saul J. Silverstein.

We thank Christos Panagiotidis and Tarik Soliman for their critical comments on the manuscript.

REFERENCES

1. **Ackermann, M., D. K. Braun, L. Pereira, and B. Roizman.** 1984. Characterization of herpes simplex virus 1 alpha proteins 0, 4, and 27 with monoclonal antibodies. J. Virol. **52:**108–118.
2. **Ascoli, C. A., and G. G. Maul.** 1991. Identification of a novel nuclear domain. J. Cell Biol. **112:**785–795.
3. **Ausubel, F., R. Brent, R. Kingston, D. Moore, J. Seidman, J. Smith, and K. Struhl.** 1995. Current protocols in molecular biology. John Wiley & Sons, Inc., New York, N.Y.
4. **Barlow, P. N., B. Luisi, A. Milner, M. Elliott, and R. Everett.** 1994. Structure of the C_3HC_4 domain by 1H-nuclear magnetic resonance spectroscopy. J. Mol. Biol. **237:**201–211.
5. **Bohenzky, R. A., A. G. Papavassiliou, I. H. Gelman, and S. Silverstein.** 1993. Identification of a promoter mapping within the reiterated sequences that flank the herpes simplex virus type 1 UL region. J. Virol. **67:**632–642.
6. **Borden, K. L. B., M. Boddy, J. Lally, N. J. O'Reilly, S. Martin, K. Howe, E. Solomon, and P. S. Freemont.** 1995. The solution structure of the RING finger domain from the acute promyelocytic leukaemia proto-oncoprotein PML. EMBO J. **14:**1532–1541.
7. **Brasier, A. R., J. E. Tate, and J. F. Habener.** 1989. Optimized use of the firefly luciferase assay as a reporter gene in mammalian cell lines. BioTechniques **7:**1116–1122.
8. **Cai, W., and P. A. Schaffer.** 1991. A cellular function can enhance gene expression and plating efficiency of a mutant defective in the gene for ICP0, a transactivating protein of herpes simplex virus type 1. J. Virol. **65:**4078–4090.
9. **Cai, W., and P. A. Schaffer.** 1989. Herpes simplex virus type 1 ICP0 plays a critical role in the de novo synthesis of infectious virus following transfection of viral DNA. J. Virol. **63:**4579–4589.
10. **Cai, W., and P. A. Schaffer.** 1992. Herpes simplex virus type 1 ICP0 regulates expression of immediate-early, early, and late genes in productively infected cells. J. Virol. **66:**2904–2915.
11. **Chen, J., and S. Silverstein.** 1992. Herpes simplex viruses with mutations in the gene encoding ICP0 are defective in gene expression. J. Virol. **66:**2916–2927.
12. **Chen, J., X. Zhu, and S. Silverstein.** 1991. Mutational analysis of the sequence encoding ICP0 from herpes simplex virus type-1. Virology **180:**207–220.
13. **Clements, J. B., R. J. Watson, and N. M. Wilkie.** 1977. Temporal regulation of herpes simplex virus type 1 transcription: location of transcripts on the viral genome. Cell. **12:**275–285.
14. **DeLuca, N. A., A. M. McCarthy, and P. A. Schaffer.** 1985. Isolation and characterization of deletion mutants of herpes simplex virus type 1 in the gene encoding immediate-early regulatory protein ICP4. J. Virol. **56:**558–570.
15. **Dixon, R. F., and P. A. Schaffer.** 1980. Fine-structure mapping and functional analysis of temperature-sensitive mutants in the gene encoding the herpes simplex virus type 1 immediate-early protein VP175. J. Virol. **36:**189–203.
16. **DuBridge, R. B., P. Tang, H. C. Hsia, L. Phaik-Mooi, J. H. Miller, and M. P. Calos.** 1987. Analysis of mutation in human cells by using an Epstein-Barr virus shuttle system. Mol. Cell. Biol. **7:**379–387.
17. **Elshiekh, N. A., E. Harris-Hamilton, and S. L. Bachenheimer.** 1991. Differential dependence of herpes simplex virus immediate-early gene expression on de novo-infected cell protein synthesis. J. Virol. **65:**6430–6437.
18. **Everett, R., P. O'Hare, D. O'Rourke, P. Barlow, and A. Orr.** 1995. Point mutations in the herpes simplex virus type 1 Vmw110 RING finger helix affect activation of gene expression, viral growth, and interaction with PML-containing nuclear structures. J. Virol. **69:**7339–7344.
19. **Everett, R. D.** 1988. Analysis of the functional domains of herpes simplex virus type 1 immediate-early polypeptide Vmw110. J. Mol. Biol. **202:**87–96.
20. **Everett, R. D.** 1989. Construction and characterization of herpes simplex virus type 1 mutants with defined lesions in immediate early gene 1. J. Gen. Virol. **70:**1185–1202.
21. **Everett, R. D.** 1987. A detailed mutational analysis of VMW110, a trans-acting transcriptional activator encoded by herpes simplex virus type 1. EMBO J. **6:**2069–2076.
22. **Everett, R. D.** 1986. The products of herpes simplex virus type 1 (HSV-1) immediate early genes 1, 2, and 3 can activate HSV-1 gene expression in trans. J. Gen. Virol. **68:**2507–2513.
23. **Everett, R. D.** 1984. Trans-activation of transcription by herpes virus products: requirement for two HSV-1 immediate-early polypeptides for maximum activity. EMBO J. **3:**3135–3141.
24. **Everett, R. D., P. Barlow, A. Milner, B. Luisi, A. Orr, G. Hope, and D. Lyon.** 1993. A novel arrangement of zinc-binding residues and secondary structure in the C_3HC_4 motif of an alpha herpes virus protein family. J. Mol. Biol. **234:**1038–1047.
25. **Everett, R. D., and G. G. Maul.** 1994. HSV-1 IE protein Vmw110 causes redistribution of PML. EMBO J. **13:**5062–5069.
26. **Fraser, N. W., T. M. Block, and J. G. Spivack.** 1992. The latency-associated transcripts of herpes simplex virus: RNA in search of function. Virology **191:**1–8.
27. **Freemont, P. S.** 1993. The RING finger. A novel protein sequence related to the zinc finger. Ann. N.Y. Acad. Sci. **684:**174–192.
28. **Freemont, P. S., I. M. Hanson, and J. Trowsdale.** 1991. A novel cysteine-rich sequence motif. Cell. **64:**483–484.
29. **Gelman, I., and S. Silverstein.** Unpublished data.
30. **Gelman, I. H., and S. Silverstein.** 1986. Coordinate regulation of herpes simplex virus gene expression is mediated by the functional interaction of two immediate early gene products. J. Mol. Biol. **191:**395–409.
31. **Gelman, I. H., and S. Silverstein.** 1987. Herpes simplex virus immediate-early promoters are responsive to virus and cell *trans*-acting factors. J. Virol. **61:**2286–2296.
32. **Gelman, I. H., and S. Silverstein.** 1985. Identification of immediate early genes from herpes simplex virus that transactivate the virus thymidine kinase gene. Proc. Natl. Acad. Sci. USA **82:**5265–5269.
33. **Harris, R. A., R. D. Everett, X. Zhu, S. Silverstein, and C. M. Preston.** 1989. The herpes simplex virus (HSV) immediate-early protein $V_{MW}110$ reactivates latent HSV-2 in an in vitro latency system. J. Virol. **63:**3513–3515.
34. **Hay, R. T., and J. Hay.** 1980. Properties of herpesvirus-induced immediate early polypeptides. Virology **104:**230–234.
35. **Hirt, B.** 1967. Selective extraction of polyoma DNA from infected mouse cell cultures. J. Mol. Biol. **26:**365–369.
36. **Holland, L. E., K. P. Anderson, C. Shipman, and E. K. Wagner.** 1980. Viral DNA synthesis is required for the efficient expression of specific herpes simplex virus type 1 mRNA species. Virology **101:**10–24.
37. **Honess, R. W., and B. Roizman.** 1974. Regulation of herpesvirus macromolecular synthesis. I. Cascade regulation of the synthesis of three groups of viral proteins. J. Virol. **14:**8–19.
38. **Honess, R. W., and B. Roizman.** 1975. Regulation of herpesvirus macromolecular synthesis: sequential transition of polypeptide synthesis requires functional viral polypeptides. Proc. Natl. Acad. Sci. USA **72:**1276–1280.
39. **Kawaguchi, Y., and B. Roizman.** 1997. Interaction of herpes simplex virus type 1 α regulatory protein ICP0 with elongation factor 1δ: ICP0 affects translational machinery. J. Virol. **71:**1019–1024.

40. **Kramer, M., and D. Coen.** 1995. Quantification of transcripts from the ICP4 and thymidine kinase genes in mouse ganglia latently infected with herpes simplex virus. J. Virol. **69:**1389–1399.
41. **Laemmli, U. K.** 1970. Cleavage of structural proteins during the assembly of the head of bacteriophage T4. Nature **227:**680–685.
42. **Leopardi, R., N. Michael, and B. Roizman.** 1995. Repression of the herpes simplex virus type 1 α4 gene by its gene product (ICP4) within the context of the viral genome is conditioned by the distance and stereoaxial alignment of the ICP4 DNA binding site relative to the TATA box. J. Virol. **69:**3042–3048.
43. **Lium, E. K., C. A. Panagiotidis, X. Wen, and S. J. Silverstein.** 1996. Repression of the α0 gene by ICP4 during a productive herpes simplex virus infection. J. Virol. **70:**3488–3496.
44. **Lukonis, C., J. Burkham, and S. Weller.** 1997. Herpes simplex virus type 1 prereplicative sites are a heterogeneous population: only a subset are likely to be precursors to replication compartments. J. Virol. **71:**4771–4781.
45. **Maul, G., H. Guldner, and J. Spivack.** 1993. Modification of discrete nuclear domains induced by herpes simplex virus type 1 immediate early gene 1 product. J. Gen. Virol. **74:**2679–2690.
46. **Maul, G. G., and R. D. Everett.** 1994. The nuclear location of PML, a cellular member of the C3HC4 zinc-binding domain protein family, is rearranged during herpes simplex virus infection by the C3HC4 viral protein ICP0. J. Gen. Virol. **75:**1223–1233.
47. **McCarthy, A. M., L. McMahan, and P. A. Schaffer.** 1989. Herpes simplex virus type 1 ICP27 deletion mutants exhibit altered patterns of transcription and are DNA deficient. J. Virol. **63:**18–27.
48. **Moriuchi, H., M. Moriuchi, S. E. Straus, and J. I. Cohen.** 1993. Varicella zoster virus (VZV) open reading frame 61 protein transactivates VZV gene promoters and enhances the infectivity of VZV DNA. J. Virol. **67:**4290–4295.
49. **Nagpal, S., and J. M. Ostrove.** 1991. Characterization of a potent varicella-zoster virus-encoded *trans*-repressor. J. Virol. **65:**5289–5296.
50. **Numoto, M., O. Niwa, J. Kaplan, K. Wong, K. Merrell, K. Kaniya, K. Yanagihara, and K. Calame.** 1993. Transcriptional repressor ZF5 identifies a new conserved domain in zinc finger proteins. Nucleic Acids Res. **21:**3767–3775.
51. **O'Hare, P., and G. S. Hayward.** 1985. Evidence for a direct role for both the 175,000- and 110,000-molecular-weight immediate-early proteins of herpes simplex virus in the transactivation of delayed-early promoters. J. Virol. **53:**751–760.
52. **O'Hare, P., and G. S. Hayward.** 1985. Three *trans*-acting regulatory proteins of herpes simplex virus modulate immediate-early gene expression in a pathway involving positive and negative feedback regulation. J. Virol. **56:**723–733.
53. **Panagiotidis, C., and S. Silverstein.** Unpublished data.
54. **Panagiotidis, C. A., S. C. Huang, and E. S. Canellakis.** 1995. Relationship of the expression of the S20 and L34 ribosomal proteins to polyamine biosynthesis in *Escherichia coli*. Int. J. Biochem. Cell Biol. **27:**157–168.
55. **Panagiotidis, C. A., E. K. Lium, and S. J. Silverstein.** 1997. Physical and functional interactions between herpes simplex virus immediate-early proteins ICP4 and ICP27. J. Virol. **71:**1547–1557.
56. **Pereira, L., M. H. Wolff, M. Fenwick, and B. Roizman.** 1977. Regulation of herpesvirus macromolecular synthesis. V. Properties of alpha polypeptides made in HSV-1 and HSV-2 infected cells. Virology **77:**733–749.
57. **Preston, C. M.** 1979. Control of herpes simplex virus type 1 mRNA synthesis in cells infected with wild-type virus or the temperature-sensitive mutant *ts*K. J. Virol. **29:**275–284.
58. **Rice, S. A., and D. M. Knipe.** 1988. Gene-specific trans-activation by the herpes simplex virus type 1 alpha protein ICP27. J. Virol. **62:**3814–3823.
59. **Rice, S. A., M. C. Long, V. Lam, and C. A. Spencer.** 1994. RNA polymerase II is aberrantly phosphorylated and localized to viral replication compartments following herpes simplex virus infection. J. Virol. **68:**988–1001.
60. **Roberts, M. S., A. Boundy, P. O'Hare, M. C. Pizzorno, D. M. Ciufo, and G. S. Hayward.** 1988. Direct correlation between a negative autoregulatory response element at the cap site of the herpes simplex virus type 1 IE175 (α4) promoter and a specific binding site for the IE175 (ICP4) protein. J. Virol. **62:**4307–4320.
61. **Roizman, B., and A. Sears.** 1993. The human herpes viruses. Raven Press, New York, N.Y.
62. **Sacks, W. R., C. C. Greene, D. P. Aschman, and P. A. Schaffer.** 1985. Herpes simplex virus type 1 ICP27 is an essential regulatory protein. J. Virol. **55:**796–805.
63. **Sacks, W. R., and P. A. Schaffer.** 1987. Deletion mutants in the gene encoding the herpes simplex virus type 1 immediate-early protein ICP0 exhibit impaired growth in cell culture. J. Virol. **61:**829–839.
64. **Samaniego, L., N. Wu, and N. A. DeLuca.** 1997. The herpes simplex virus immediate-early protein ICP0 affects transcription from the viral genome and infected-cell survival in the absence of ICP4 and ICP27. J. Virol. **71:**4614–4625.
65. **Samaniego, L. A., A. L. Webb, and N. A. DeLuca.** 1995. Functional interactions between herpes simplex virus immediate-early proteins during infection: gene expression as a consequence of ICP27 and different domains of ICP4. J. Virol. **69:**5705–5715.
66. **Smiley, J.** 1980. Construction in vitro and rescue of a thymidine kinase deficient deletion mutant of herpes simplex virus. Nature **285:**333–335.
67. **Soliman, T., R. Sandri-Goldin, and S. Silverstein.** Shuttling between the nucleus and cytoplasm of the herpes simplex virus type 1 regulatory protein ICP27 mediates the expression of late proteins. J. Virol., in press.
68. **Spatz, S. J., E. C. Nordby, and P. C. Weber.** 1996. Mutational analysis of ICP0R, a transrepressor protein created by alternative splicing of the ICP0 gene of herpes simplex virus type 1. J. Virol. **70:**7360–7370.
69. **Stevens, J. G., E. K. Wagner, G. Devi-Rao, M. L. Cook, and L. T. Feldman.** 1987. RNA complementary to a herpesvirus alpha gene mRNA is prominent in latently infected neurons. Science **235:**1056–1059.
70. **Stow, N. D., and E. C. Stow.** 1986. Isolation and characterization of a herpes simplex virus type 1 mutant containing a deletion within the gene encoding the immediate early polypeptide Vmw110. J. Gen. Virol. **67:**2571–2585.
71. **Swanstrom, R. I., K. Pivo, and E. K. Wagner.** 1974. Restricted transcription of the herpes simplex virus genome occurring early after infection and in the presence of metabolic inhibitors. Virology **66:**140–150.
72. **Towbin, H., T. Staehelin, and J. Gordon.** 1979. Electrophoretic transfer of proteins from polyacrylamide gels to nitrocellulose sheets: procedure and some applications. Proc. Natl. Acad. Sci. USA **76:**4350–4354.
73. **Uprichard, S. L., and D. M. Knipe.** 1996. Herpes simplex ICP27 mutant viruses exhibit reduced expression of specific DNA replication genes. J. Virol. **70:**1969–1980.
74. **Upton, C., L. Schiff, S. A. Rice, T. Dowdeswell, X. Yang, and G. McFadden.** 1994. A poxvirus protein with a ring finger motif binds zinc and localizes in virus factories. J. Virol. **68:**4186–4195.
75. **van Zonneveld, A. J., S. A. Curriden, and D. J. Luskutoff.** 1988. Type 1 plasminogen activator inhibitor gene: functional analysis and glucocorticoid regulation of its promoter. Proc. Natl. Acad. Sci. USA **85:**5525–5529.
76. **Watson, R. J., and J. B. Clements.** 1980. A herpes simplex type 1 function continuously required for early and late virus RNA synthesis. Nature **285:**329–330.
77. **Wigler, M., A. Pellicer, S. Silverstein, R. Axel, G. Urlaub, and L. Chasin.** 1979. DNA-mediated transfer of the adenine phosphoribosyltransferase locus into mammalian cells. Proc. Natl. Acad. Sci. USA **76:**1373–1376.
78. **Wilcox, K. W., A. Kohn, E. Sklyanskaya, and B. Roizman.** 1980. Herpes simplex virus phosphoproteins. I. Phosphate cycles on and off some viral polypeptides and can alter their affinity for DNA. J. Virol. **33:**167–182.
79. **Wirth, U. V., F. C., B. Vogt, C. Vlcek, V. Paces, and M. Schwyzer.** 1992. Immediate-early RNA 2.9 and early RNA 2.6 of bovine herpesvirus 1 are 3′ coterminal and encode a putative zinc finger transactivator protein. J. Virol. **66:**2763–2772.
80. **Yao, F., and P. Schaffer.** 1995. An activity specified by the osteosarcoma line U2OS can substitute functionally for ICP0, a major regulatory protein of herpes simplex virus type 1. J. Virol. **69:**6249–6258.
81. **Zhu, X., J. Chen, and S. Silverstein.** 1991. Isolation and characterization of a functional cDNA encoding ICP0 from herpes simplex virus type 1. J. Virol. **65:**957–960.
82. **Zhu, X., J. Chen, C. S. H. Young, and S. Silverstein.** 1990. Reactivation of latent herpes simplex virus by adenovirus recombinants encoding mutant IE-0 gene products. J. Virol. **64:**4489–4498.